International
Progress Report

IPR-07-14

Äspö Hard Rock Laboratory

LASGIT Large Scale Gas Injection Test

Hydraulic tests with surface packer systems

Thomas Nowak
Hartwig Köster
Reiner Flentje
Silvio Sanchez-Herrero
Christian Lege

Federal Institute for Geosciences and
Natural Resources, Hannover, Germany

October 2007

Svensk Kärnbränslehantering AB
Swedish Nuclear Fuel
and Waste Management Co
Box 5864
SE-102 40 Stockholm Sweden
Tel 08-459 84 00
+46 8 459 84 00
Fax 08-661 57 19
+46 8 661 57 19

Äspö Hard Rock
Laboratory

Report no.	No.
IPR-07-14	F122K
Author	Date
Thomas Nowak Hartwig Köster Reiner Flentje Silvio Sanchez-Herrero Christian Lege	October 2007
Checked by	Date
Heikki Raiko	2007-11-14
Approved	Date
Anders Sjöland	2007-11-21

Äspö Hard Rock Laboratory

LASGIT Large Scale Gas Injection Test

Hydraulic tests with surface packer systems

Thomas Nowak
Hartwig Köster
Reiner Flentje
Silvio Sanchez-Herrero
Christian Lege

Federal Institute for Geosciences and
Natural Resources, Hannover, Germany

October 2007

Keywords: Excavation, Damaged zone, Hydraulic test, Modelling, Permeability, Pulse test

Abstract

For the hydraulic characterization of the excavation damaged zone BGR has developed surface packer systems. This packer type is fixed directly on the gallery wall, for this reason it is very qualified as a tool to characterize the area that is most damaged by excavation where borehole packers are not applicable. The surface packer systems were used in the HRL Äspö in galleries that were excavated by drill and blast and by TBM, also in deposition holes. Water, air, and Helium were used as test fluid.

This report describes the surface packer equipment itself, explains the different methods for the analysis of the hydraulic tests and documents the results of these tests.

Sammanfattning

För att kunna karaktärisera de hydrauliska egenskaperna hos den störda zonen har BGR utvecklat ett system med ytpackers. Packertypen fästs direkt på bergytan, vilket gör att det är ett mycket kvalificerat verktyg för att karaktärisera det område som är mest skadat och där borrhålspackers är olämpliga. Ytpackersystemet har använts i Äspölaboratoriet i sprängda och TBM-borrade tunnlar samt i deponeringshål. Vatten, luft och helium har använts som testmedium.

Den här rapporten beskriver ytpackerutrustningen, förklarar de olika metoderna för analys av de hydrauliska testerna och dokumenterar resultaten från dessa tester.

Contents

1 Introduction

For the investigation of concepts for final disposal in crystalline formations the Swedish Nuclear Fuel and Waste Management Co (SKB) operates the Hard Rock Laboratory Äspö. According to the demand of the German Government to investigate alternative host rocks BGR has participated in numerous international projects that have been conducted in this laboratory.

One issue in this field of research is the excavation damaged zone. In crystalline formations the movement of water and gas takes place mainly on natural fractures or (micro-)cracks. In the vicinity of a cavity the formation of (micro-)cracks is controlled by the mechanical behaviour of the formation, the initial stress field, and the method of excavation.

For the hydraulic testing of the excavation damaged zone BGR has developed surface packer systems. The purpose of hydraulic testing is the determination of the permeability of the rock, whereas the term “hydraulic” refers to both liquid and gas as test fluid. The principle of testing is the monitoring of the pressure response while a test fluid with known viscosity and compressibility is extracted from or injected into a test interval. The permeability can be determined from the relationship between flow rate and pressure response. Surface packers are fixed directly on the gallery wall, for this reason this system is suitable to characterize the area that is most damaged by excavation where borehole packers are not applicable.

This report summarizes the results from the recent surface packer tests that were performed and analysed in the framework of the NF-PRO project. Test locations were in the deposition hole DA3147G01 (LASGIT), the drill and blast excavated Q-tunnel, and the TBM-excavated A-tunnel.

2 Test Locations

For the hydraulic tests in the course of the NF-PRO project mainly the rock matrix of the excavation damaged zone (EDZ) was in focus. The term “rock matrix” is used here following the approach from MARSCHALL et al. (1999) for a rock volume without visible fractures.

BGR developed surface packer systems especially for the investigation of the EDZ. As Figure 2-1 shows, classical single or double packers for hydraulic testing in boreholes are not applicable for the first centimetres of rock that are supposed to be most damaged by the excavation process.

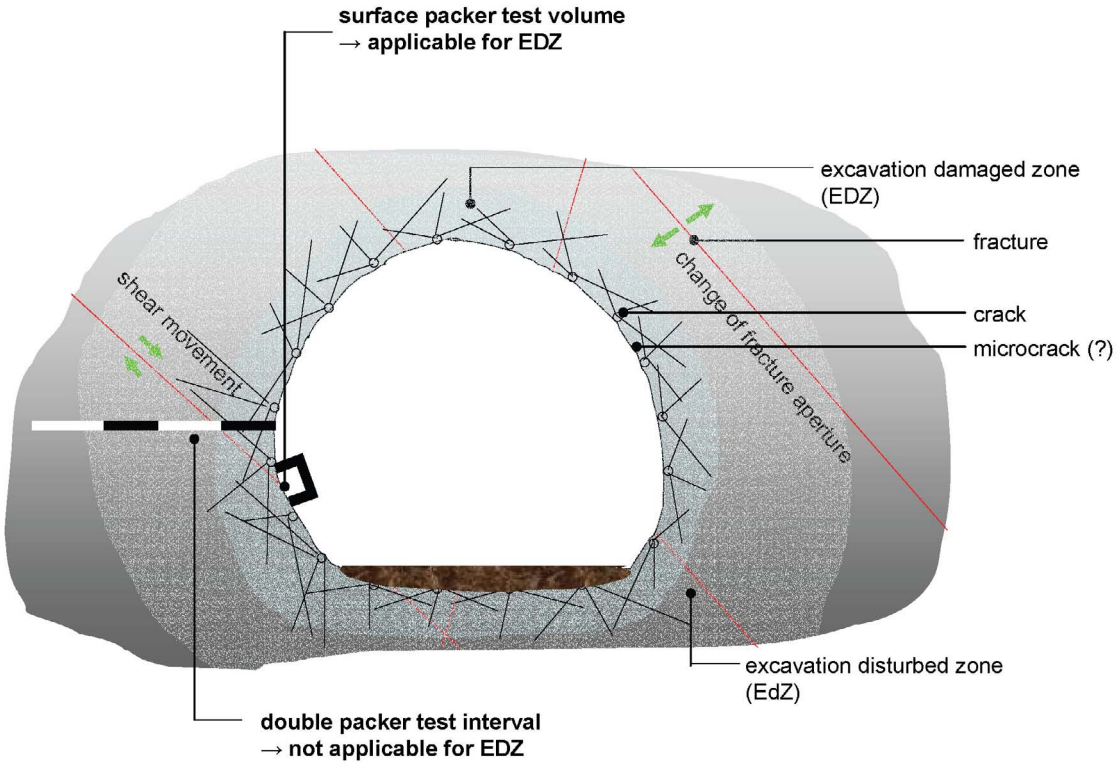

Figure 2-1. *Surface packer for investigation of the EDZ.*

The high permeability of cracks themselves that are induced by drill and blast excavation is obvious, compare Figure 2-2 left side: this photo was taken in a slot in the wall of the Q-tunnel. On the other hand, the permeability perpendicular to a crack might be very low. It is not possible to make a general statement to the permeability of the excavation damaged zone; permeability depends on direction of measurement as well as starting-point and end-point of the pathway of interest through the rock volume of interest.

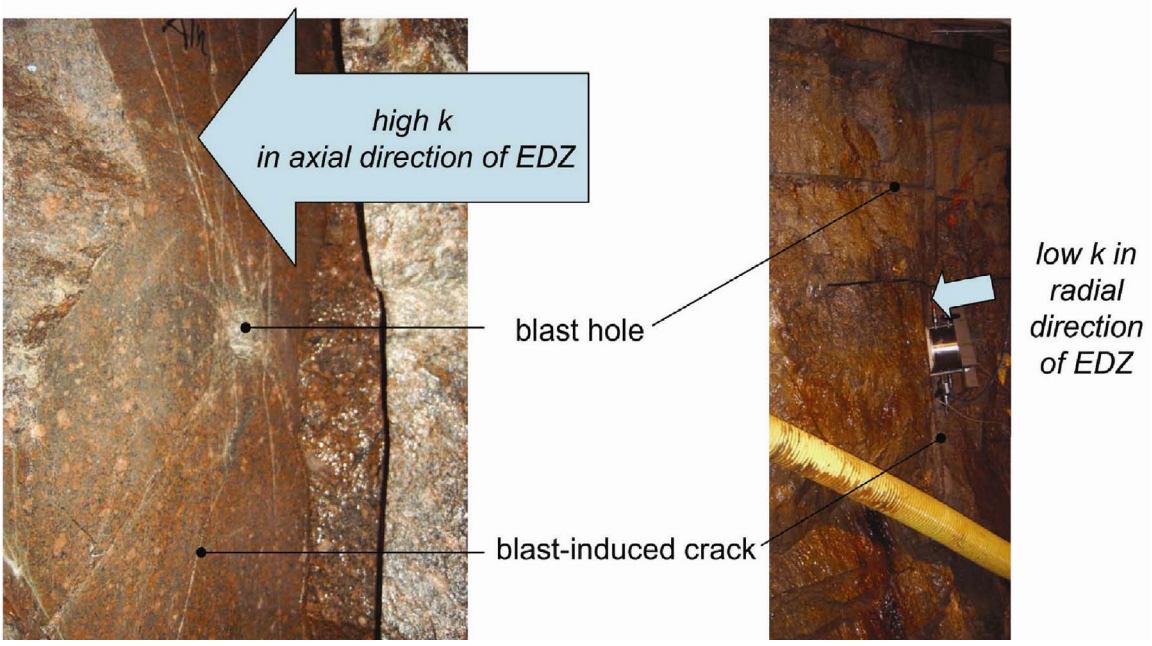

Figure 2-2. *Permeability of the excavation damaged zone.*

Hydraulic tests with surface packer systems were conducted by BGR at the HRL Äspö in deposition holes and galleries that were excavated with TBM or drill and blast. Figure 2-3 gives an overview of the locations.

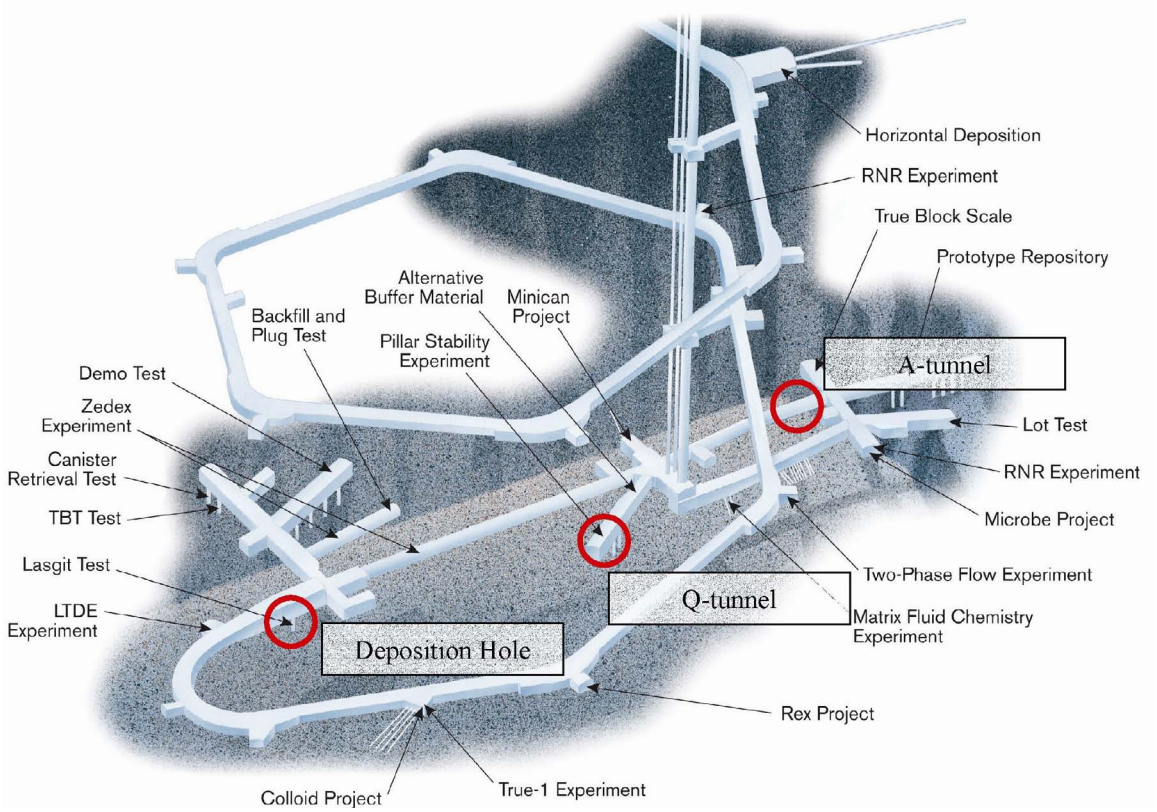

Figure 2-3. *Locations for hydraulic tests with surface packer systems at the HRL Äspö (picture taken from SKB information material and modified).*

2.1 Deposition Hole DA3147G01 (LASGIT)

For the investigation of the EDZ around deposition hole DA3147G01 BGR measured permeability with the bentonite surface packer system, which was the first in situ application of this type of sealing. For the (potentially) excavation disturbed zone (EdZ) a sub-contractor of SKB performed hydraulic measurements in surrounding boreholes which were analyzed by BGR, the results are published in HARDENBY (2004).

Tests were planned (Figure 2-4) on positions with waterbearing fractures in the deposition hole - indicated with blue circles - and on one position without visible fractures - indicated with the green circle. Local seawater was used as test fluid.

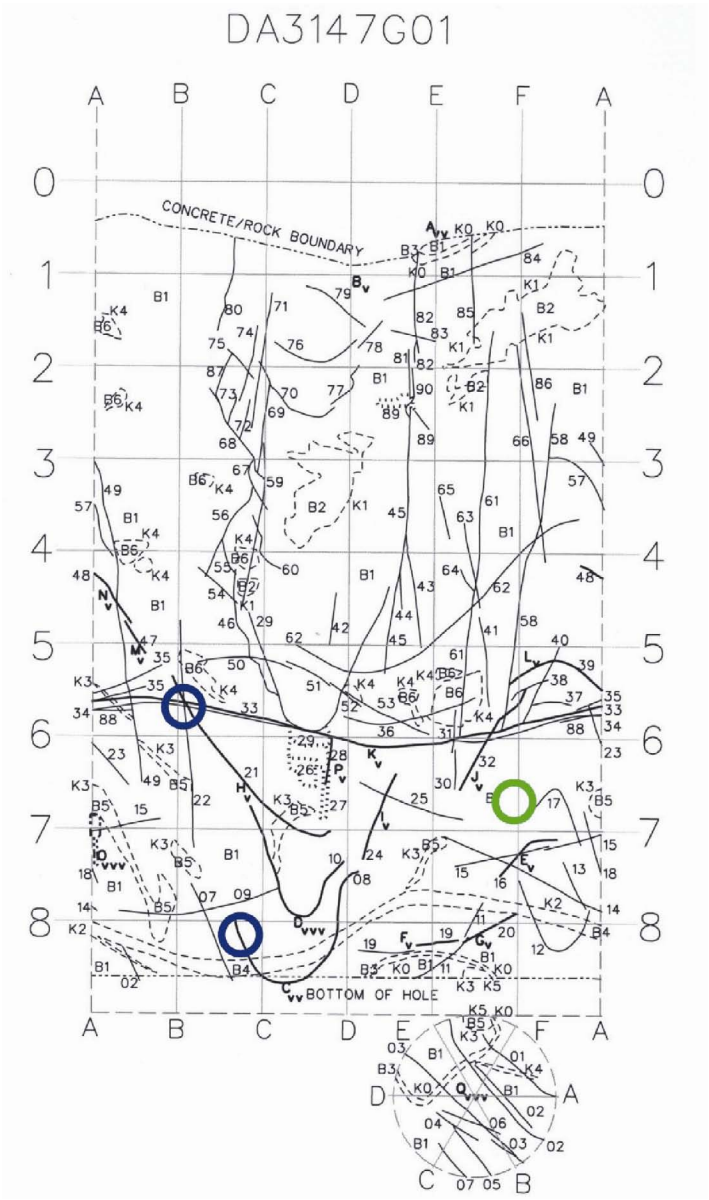

Figure 2-4. *Test plan for deposition hole DA3147G01 (LASGIT).*

The tests on the fractured positions failed: instead of swelling, the bentonite was washed out of the furrow during the hydration phase by the inflowing water from the fracture. The asperities on the wall of the deposition hole on these positions turned out to be too rough.

2.2 Q-Tunnel

For the investigation of the excavation damaged zone in a gallery excavated by drill and blast BGR measured permeability with the bentonite surface packer system at four positions in the Q-tunnel (Figure 2-5 and Figure 2-6).

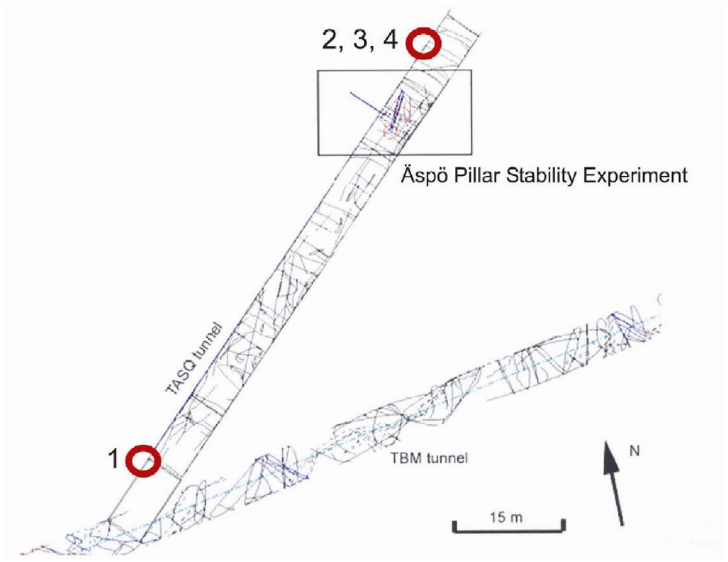

Figure 2-5. *Test locations in the Q-tunnel.*

Test No. 1 was conducted at the entrance of the Q-tunnel next to a blast hole. Test No. 2 was conducted near the end of the Q-tunnel on a (natural) fracture plane. Test No. 3 and 4 were conducted near the end of the Q-tunnel in a slot in the wall. With help of these slots which were excavated at several positions in the Q-tunnel SKB investigates different drill and blast designs for minimizing the blast induced damage. For test planning SKB provided the photo shown in Figure 2-6 right hand side: The surface of the slot was dried as to make small water inflows coming from cracks or fractures visible. The green circle indicates test location no. 3 and the blue circle the test location no. 4. A test planned on the position indicated with the dotted blue circle unfortunately failed.

Figure 2-6. *Photos of test locations in the Q-tunnel: location 1, 2, 3&4.*

2.3 A-tunnel

For the investigation of the excavation damaged zone in a gallery excavated by TBM BGR measured permeability in the A-tunnel with several configurations of the test equipment and different test fluids. Several test locations are prepared in that tunnel on positions without visible crack. Some of these locations are prepared with an additional central borehole beneath the surface packer for small scale hydraulic interference tests. Figure 2-7 shows a photo of this type of test locations on the left side and a principle sketch of the surface packer / mini packer installation. In case that micro-cracks intersect with the test location (either on the gallery wall beneath the surface packer or the wall of the central borehole) the permeability value might be increased. When a micro-crack connects both testing volumes hydraulic communication might be determined. Table 2-1 contains the length of the central borehole to the test locations described in this report; the diameter is for all 12 mm.

A first series of tests was done with the surface packer / mini packer system. While a pressure pulse was applied to the surface packer also the pressure response in the mini borehole was monitored (and vice versa). The tests were performed with gas as test fluid; two-phase-flow conditions had to be considered.

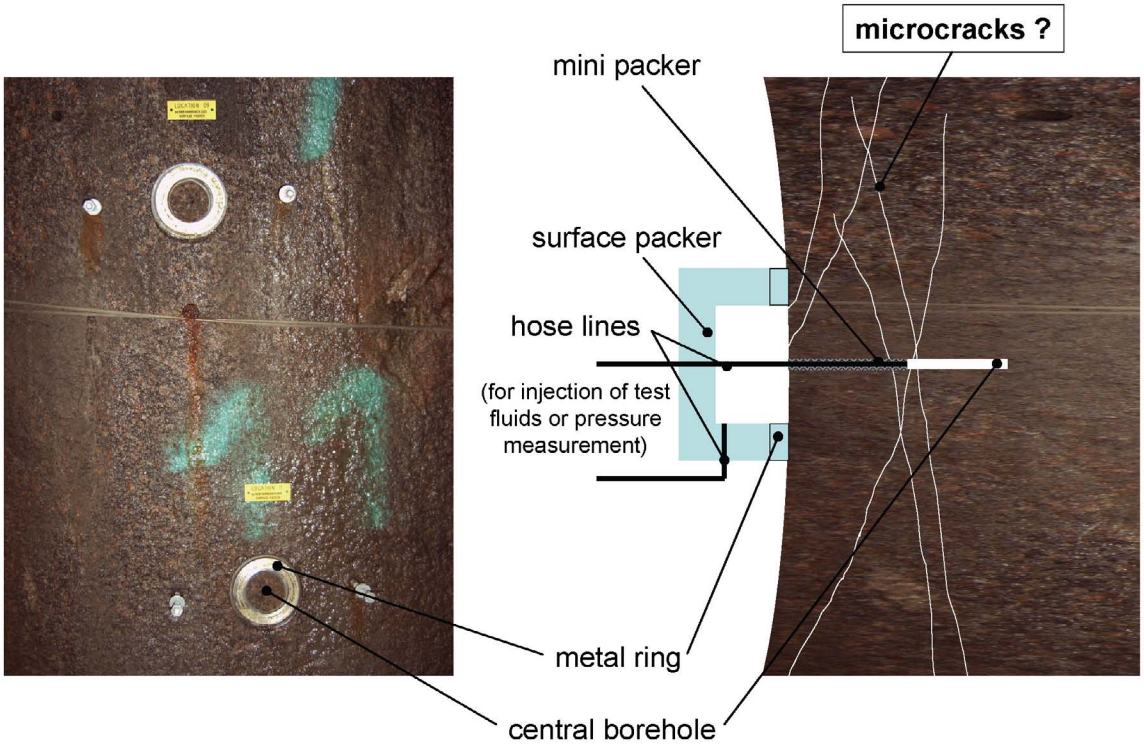

Figure 2-7. *Photo of some test locations in the A-tunnel (left) and principle sketch of the surface packer / mini packer installation (right).*

Table 2-1. Length of central borehole at locations in A-tunnel.

location	borehole length [cm]
PA3470A02	5.5
PA3473A02	5.8
PA3473A01	6.0
PA3474A01	5.8
PA3491A01	5.9
PA3492A02	5.6

In preparation of the gas tracer tests numerical modelling was performed for appropriate planning of these gas tracer tests. From these modelling calculations it became clear that the permeability value is crucial for the necessary test duration. As the tests with gas from the first test series could not have been analysed with respect to intrinsic permeability the same locations were tested with the surface packer (without mini packer) using water as test fluid. In the following these tests are denominated as the second test series.

In the third test series gas tracer tests were performed at two locations in the A-tunnel: PA3474A01 and PA3473A01. These locations were chosen on basis of the surface packer tests with gas and with water from the first and second test series. At location PA3474A01 a hydraulic communication between borehole and gallery wall had been found (compare chapter 5.3.1). The second test location PA3473A01 had been chosen as reference: like at all other locations that were tested with gas no hydraulic communication between borehole and gallery wall had been found. Tests with water on these locations had shown no significant difference with respect to permeability (compare chapter 5.3.2).

3 Surface Packer Equipment

This chapter describes mainly the surface packer itself which is principally a hollow metal cylinder fixed onto the test location. The part for data acquisition does not differ from conventional systems for hydraulic testing in boreholes.

For the first surface packer system of BGR the surface of the test location has to be smoothed (Figure 3-1) before a metal ring can be glued onto the test location.

Figure 3-1. *Preparation of a surface packer test location.*

An O-ring between surface packer and metal ring seals the void which corresponds to the test interval in a borehole. The surface packer is fixed onto the metal ring by a traverse. Water or gas can be injected into the void while the flow rate and/or pressure response is measured (Figure 3-2).

Figure 3-2. *Installation of surface packer system.*

For more detailed characterization of the first centimetres of the (potential) EDZ an additional mini borehole packer (length of packer: 35 mm) has been added to this system to perform interference test on a very small scale. Figure 3-3 shows a sketch of this modification and a photo of the equipment. This system was used for the first series of tests in the A-tunnel (compare chapter 2.3). The test volume can be derived from the data in Table 3-2 (pressure pulse in surface packer) and Table 2-1 (pressure pulse in central borehole).

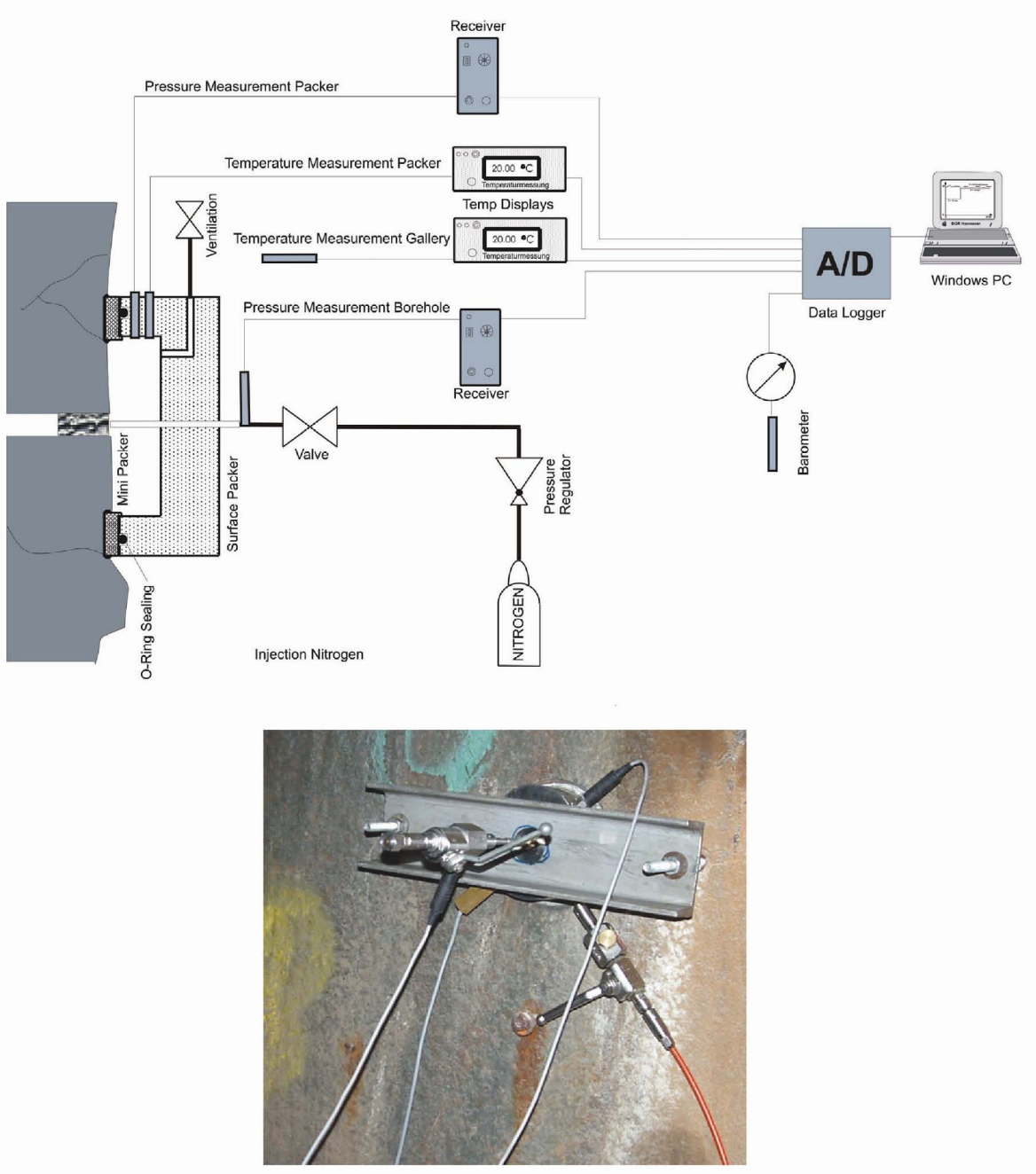

Figure 3-3. *Surface packer / mini packer system: sketch and photos.*

The second surface packer system uses bentonite as sealing material instead of the metal ring / O-ring. A preparation of the test location by smoothing the surface is not necessary for this type of sealing. Before fixing this packer type on the test location bentonite is filled (as unsaturated powder) into a furrow in the surface packer (Figure 3-4). When the packer is fixed, water is filled into the packer. When the water comes into contact with the bentonite it causes the swelling of the bentonite which then seals the remaining gap between the surface of the test location and the packer. This equipment was used in the deposition hole DA3147G01 (compare chapter 2.1) and in the Q-tunnel (compare chapter 2.2). The (different) test volumes can be found in Table 3-1.

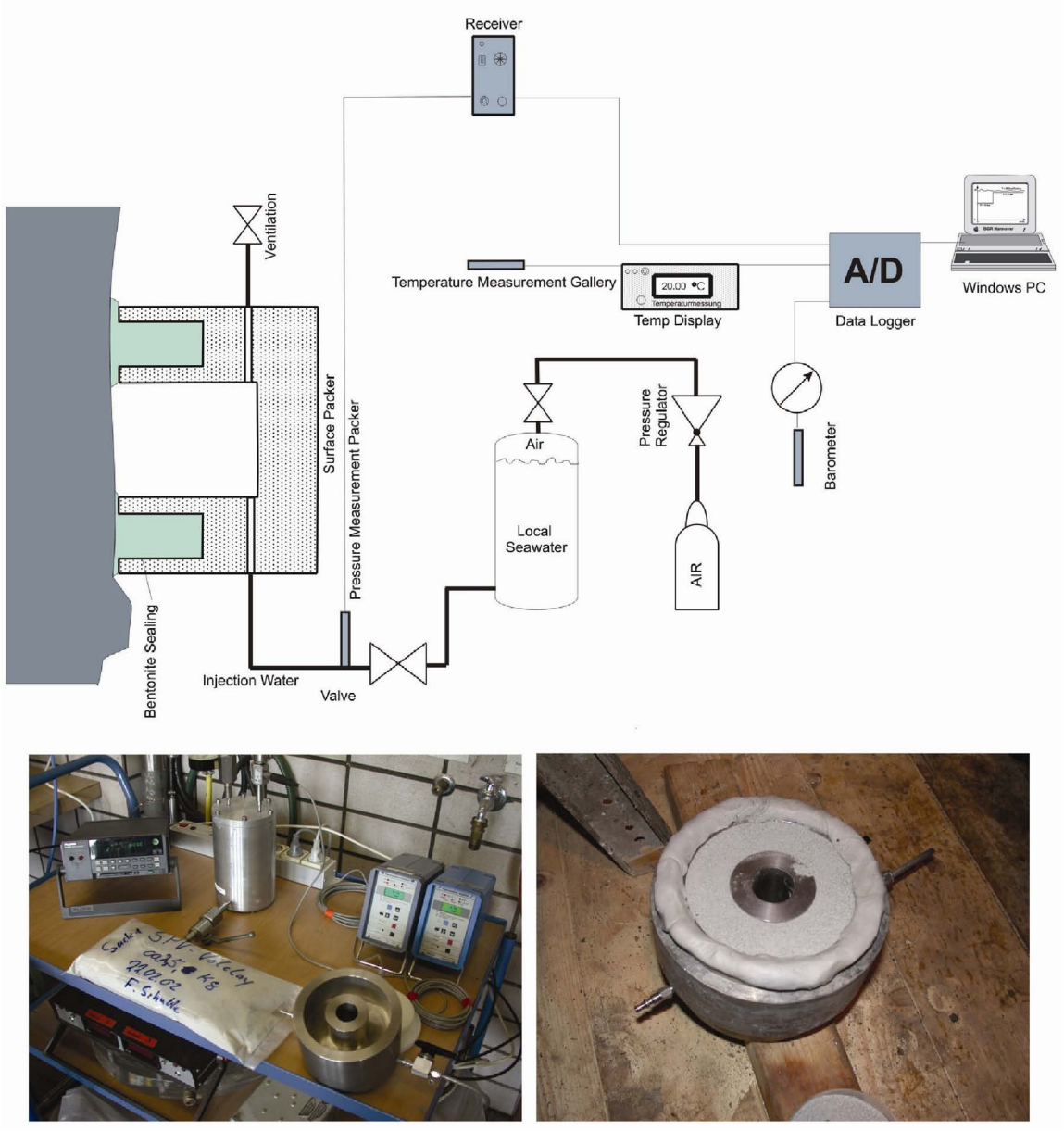

Figure 3-4. *Surface packer with bentonite sealing: sketch and photos.*

Table 3-1. Testing volume for the surface packer with bentonite sealing.

compound	volume [cm^3]	
	dep. hole	Q-tunnel
pressure vessel (inner diameter 7.6 cm, inner height 17 cm)	771.2	771.2
hose line (inner diameter 0.4 cm, length 1318 cm / 220 cm)	165.6	27.6
surface packer (inner diameter 3 cm / 4 cm, inner height 9 cm / 8 cm)	63.6	100.5
sum	1000.4	899.3

Figure 3-5 shows a sketch of the equipment for the tests with the surface packer (without mini packer) using water as test fluid. This configuration was in use for the second series of tests in the A-tunnel (compare chapter 2.3).

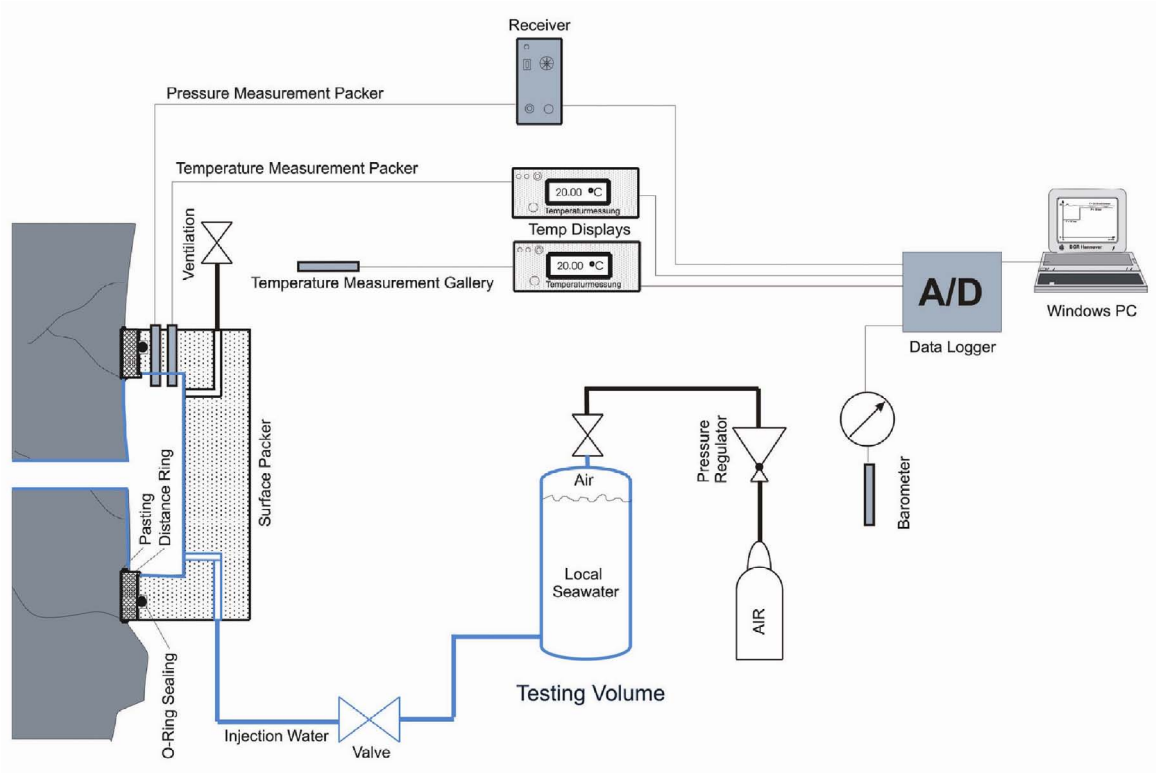

Figure 3-5. *Sketch of the surface packer system for hydraulic tests in the A-tunnel with water.*

The tests were performed as pulse tests. In the tests described in this report the volume of the pressure vessel remained connected to the surface packer and was therefore part of the testing volume (marked with the blue line). This approach was necessary because of the very low compressibility of water. The testing volume was assembled as indicated in Table 3-2. The small, varying contribution to the testing volume from the small central borehole was not taken into account.

The surface packer equipment that was used for the gas tracer tests is essentially the same as for the hydraulic surface packer tests with gas (compare Figure 3-3). The borehole was pressurized with Helium instead of air like in a pulse test and pressure in the borehole was monitored. The surface packer was installed as usual, but instead of the pressure sensor in the surface packer a small tube was connected in which the sensor hose line from the Helium detector (Leybold UL 200) ends.

The Helium detector must be operated at (near) zero overpressure. The measured value was a Helium leaking rate (unit: 100 Pa l / s). A pump in the Helium detector drew a constant gas flow through the sensor hose line. The low pressure into the sensor hose line remained about constant during the tracer test (11 Pa). The measurement of Helium leaking rate had to be stopped at regular intervals for maintenance (checking oil level of pump and flushing the device with air to clear it from Helium that might have accumulated). Figure 3-6 shows a sketch of the equipment for the tracer tests with the surface packer / mini packer using Helium as tracer.

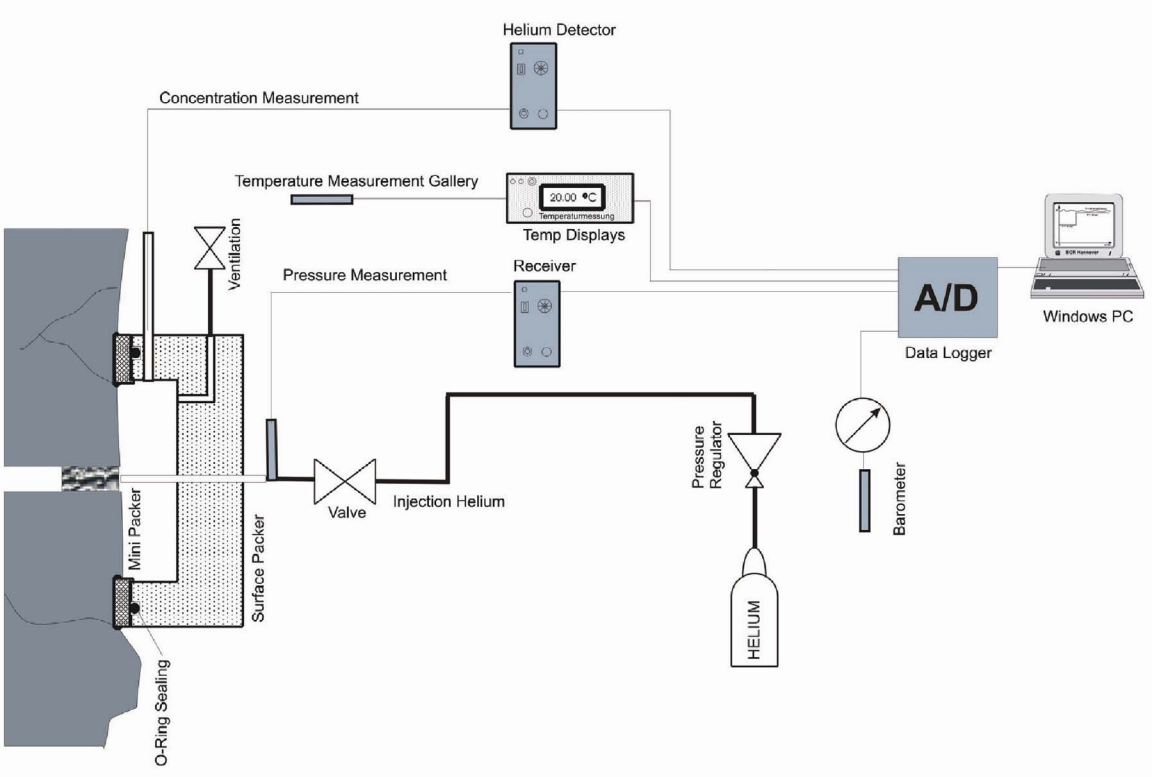

Figure 3-6. *Sketch of the surface packer system for tracer tests in the A-tunnel with Helium.*

Helium was injected into the borehole and the Helium leaking rate was measured. It is important to notice that the gas flow into the sensor hose line was a mixture of air from the gallery and the air below the surface packer. In the following the Helium leaking rate is converted into a volumetric Helium concentration of the gas flow into the sensor hose line.

Table 3-2. Testing volume for the surface packer / mini packer system.

compound	**volume [cm³]**
pressure vessel (inner diameter 7.6 cm, inner height 17 cm)	771.2
hose line (inner diameter 0.4 cm, length 232 cm)	29.2
surface packer (inner diameter 9 cm, inner height 2 cm)	127.2
sum	927.6

4 Test Analysis

The purpose of hydraulic testing is the determination of the permeability of the rock. The principle of hydraulic testing is the monitoring of the pressure response while a test fluid with known viscosity and compressibility is extracted from or injected into a test interval of a borehole or into another defined test volume that is connected to the rock, for example the surface packer.

In case of low permeability pulse tests are the test type of choice. In this kind of hydraulic test a certain pressure is build up fast in the test interval. Then the test interval is shut in and the pressure evolution is monitored. The permeability of the rock is determined by comparing the measured evolution of pressure with evolutions of pressure that are calculated for different values of permeability.

For some classical (simple) types of hydraulic tests in boreholes analytical solutions are available. For hydraulic tests with surface packer systems analytical solutions are not available, numerical modeling is necessary.

4.1 Numerical Analysis for Hydraulic Tests with the Surface Packer

All tests with BGR's surface packer systems are analyzed numerically with the finite element code (Geosys/)RockFlow; two-phase flow is generally considered both in the tests with gas as test fluid and also in the tests with water as test fluid.

Two fluid phases exist in the testing volume and need to be represented due to their different values of compressibility. Also in the tests with water some gas remains in the testing volume inevitably, but nevertheless water is the only fluid phase that is assumed to cause the pressure reduction in the testing volume by flowing into the rock.

For the testing volume the initial pulse pressure has been used as initial condition, and for the rock the pressure in the gallery as initial condition. Only boundary condition for pressure is the pressure in the gallery as indicated in Figure 4-1, saturation values can develop freely. In the tests with gas the complete testing volume is gas saturated. In the tests with water the inevitable gas in the testing volume is considered with the initial conditions for saturation: gas saturated at the top of the model, water saturated the rest.

Figure 4-1 shows (as an example) the axially symmetric numerical model of the tests with water in the A-tunnel; the numerical models for other test locations and geometries are similar. The pressure vessel and the surface packer are the part on the top (marked with blue colour, compare Figure 3-5). The exact geometric representation of the pressure vessel is not necessary, only its volume needs to be represented. The areas where the test fluid can enter the rock (underneath the surface packer and via the wall of the central borehole) are represented with their correct geometry.

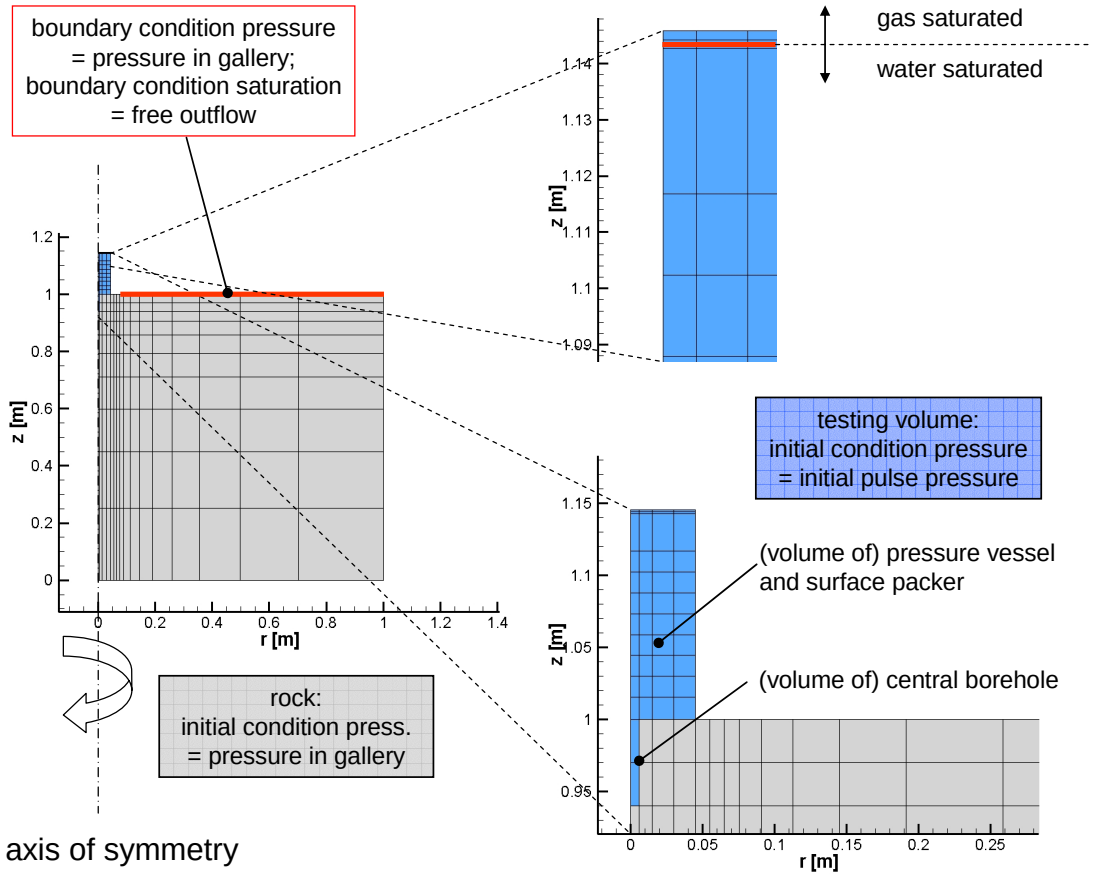

Figure 4-1. *Numerical model of the surface packer tests (example: A-tunnel).*

Figure 4-2 shows (as an example) the pressure distribution in a part of the model for the test with water on location PA3473A01 (compare chapter 5.3.2) after about 8 hours. The numbers on the contour lines are the pressure values in Pascal. For the test analysis the porosity of the rock was set to 0.2 % in the calculation and the permeability was varied; the permeability value for the test location is obtained by comparison of measured pressure evolution with calculated pressure evolution; a more detailed description can be found in chapter 5.3.2 with exemplary measured and calculated data.

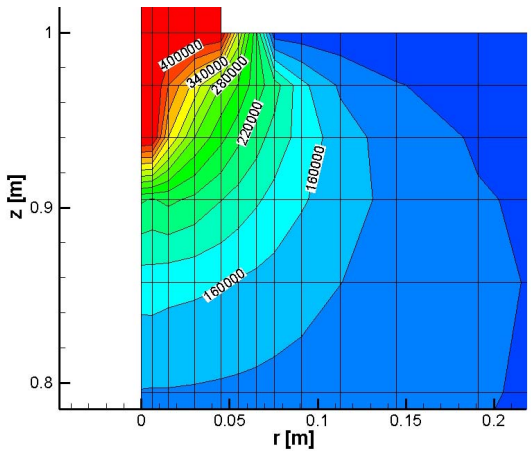

Figure 4-2. *Result for hydraulic tests: distribution plots.*

4.2 Numerical Analysis of Gas Tracer Tests with the Surface Packer

For the analysis of the tracer tests two-phase flow and conservative transport of the gas tracer in the gas phase was considered. Figure 4-3 shows the axially symmetric numerical model of the tests.

For the borehole (marked with blue colour) the initial pulse pressure was used as initial condition, and for the rock the pressure in the gallery as initial condition.

With respect to Helium volume concentration in the gas phase the initial concentration in the borehole was set depending on the initial pulse pressure p_{pulse}: it is the partial pressure of Helium (initial measured Helium concentration $c_{He,i}$ multiplied with the pressure in the gallery p_{gal} plus the pressure difference p_{pulse} - p_{gal} caused by the pressure pulse with Helium, concentration equal 1) divided by the initial pulse pressure. The initial Helium volume concentration in the gas phase within the rock volume was set according to the measured volumetric Helium concentration of the gas flow into the sensor hose line before the pressure pulse was initiated.

Boundary conditions for pressure were the pressure in the gallery at the wall and below the surface packer, compare Figure 4-3; saturation values could develop freely.

The surface packer is pictured, but not part of the FE-mesh. For the test analysis the calculated flow of gas $Q_{g,SF}$ at the nodes that represent the area below the surface packer was used together with the calculated volumetric concentration of Helium in that outflux $c_{He,SF}$: the flow of gas multiplied with the volumetric Helium concentration results in the Helium flow rate into the surface packer. The Helium detector draws a constant gas flow Q_{Det} through the sensor hose line (compare chapter 3), the measured Helium leaking rate is for a mixture of gas from the gallery (with the initial Helium concentration $c_{He,i}$) and from the surface packer. The Helium leaking rate LR_{calc} derived from the modelling calculations was calculated according to following equation:

$$LR_{calc} = (Q_{Det} - Q_{g,SF}) * c_{He,i} * p_{gal} + Q_{g,SF} * c_{He,SF} * p_{gal}$$

From this value the volumetric Helium content in the gas that is drawn through the sensor hose line by the detector can be calculated easily.

For the test analysis the porosity n of the rock was set to 0.2 %.

In combination with the measured permeabilities with water (compare chapter 5.3.2) and an assumption to the course of the two-phase flow parameters capillary pressure and relative permeabilities for water and gas the initial saturation with gas can be estimated. Figure 4-4 shows two data sets: one is a van Genuchten data set and the other set was given by the University of Catalonia to describe the granite at the Grimsel Test Site for the FEBEX in situ experiment. The parameters from UPC give a higher gas entry pressure.

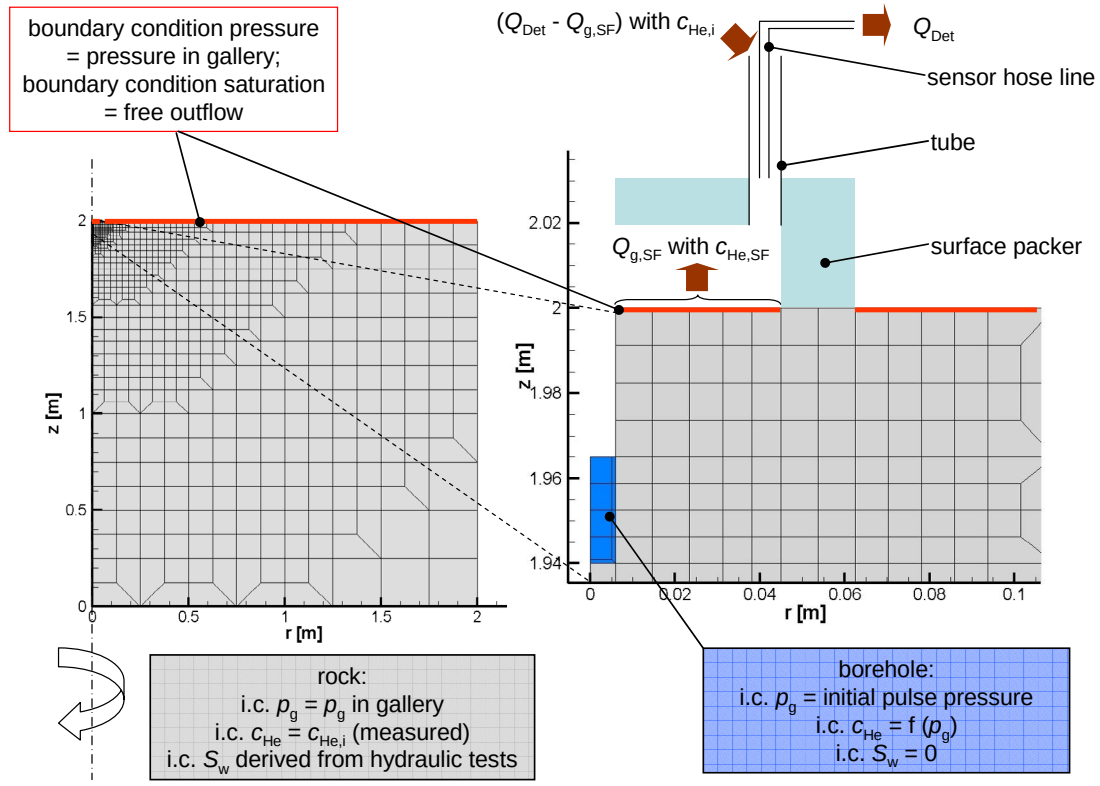

Figure 4-3. *Numerical model of the tracer tests.*

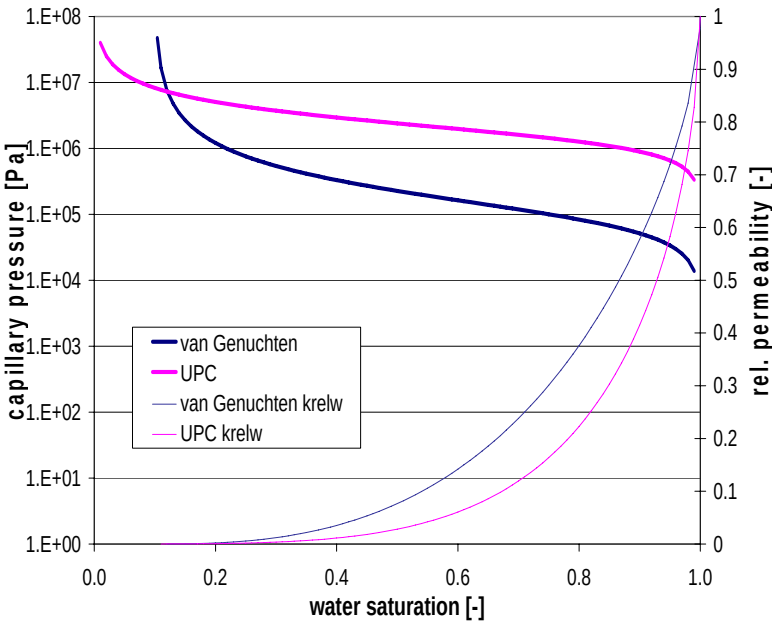

van Genuchten:

$$p_c = \frac{\rho g}{\alpha}\left(\left(\frac{S - S_{res}}{S_{max} - S_{res}}\right)^{\frac{1}{m}} - 1\right)^{\frac{1}{n}}$$

$$k_{relw} = \left(\frac{S - S_{res}}{S_{max} - S_{res}}\right)^{2}\left(1 - \left(1 - \left(\frac{S - S_{res}}{S_{max} - S_{res}}\right)^{\frac{1}{m}}\right)^{m}\right)$$

S_{res} = 0.1

S_{max} = 1.0

m = 0.468

α = 0.103 [1/m]

UPC:

$p_c = 1.74(S_w^{-1.68} - 1)^{0.405}$

$k_{relw} = S_w^{0.5}[1-(1-S_w^{1.68})^{0.595}]^2$

Figure 4-4. *Dependence of capillary pressure and relative water permeability on water saturation for crystalline rock matrix.*

The diffusion coefficient D for Helium in the gas phase was varied in the calculations for each test between a maximum value of $1.8 \cdot 10^{-6}$ m²/s and a minimum value of 10^{-7} m²/s according to experimental values from MAARANEN et al. (2001) on Äspö rock samples ($D_e = D * n/\tau$ with τ as tortuosity): they found a maximum value of $3.6 \cdot 10^{-9}$ m^2/s and a minimum value of $2 \cdot 10^{-10}$ m^2/s for the effective diffusion coefficient D_e (porosity about 0.2 %).

The longitudinal dispersion length was set to 0.0035 m which is one tenth of the closest distance between borehole and gallery wall beneath surface packer. The transversal dispersion length has been set to 0.00035 m which is one tenth of the longitudinal dispersion length.

As an example Figure 4-5 shows on the left hand side a contour plot for gas pressure (flood) and volumetric Helium content in the gas phase (lines) in the numerical model for the test on location PA3473A01 after 100 hours. The right hand side of that figure shows a contour plot for gas saturation and qualitatively the gas flow.

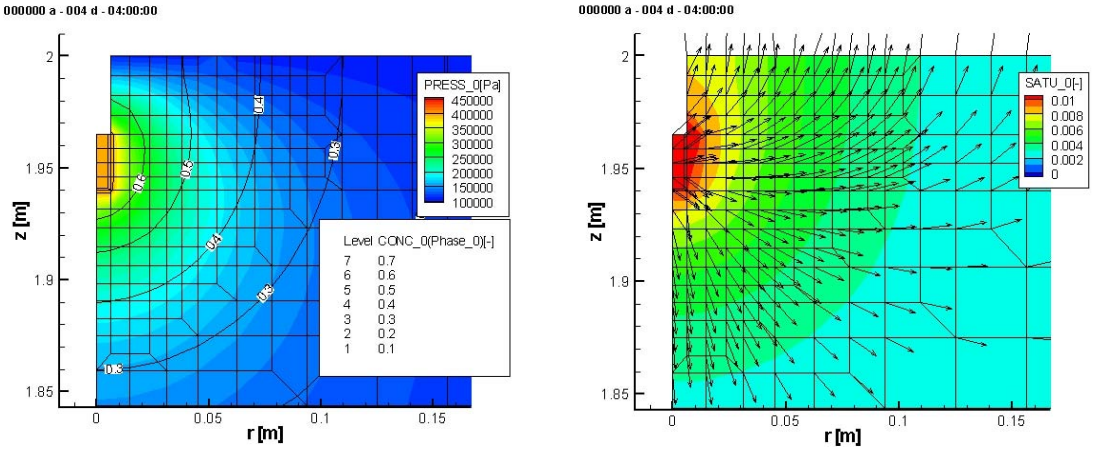

Figure 4-5. *Results for tracer tests: distribution plots.*

4.3 Analytical Analysis for Hydraulic Tests with the Mini Packer

Beneath the analysis as tracer test the measured pressure evolutions in the borehole were analyzed with an analytical method for one-phase flow as pulse tests.

The relationship between pressure evolution and permeability is described with the diffusivity equation:

$$\frac{\partial^2 p}{\partial r^2} + \frac{1}{r}\frac{\partial p}{\partial r} = \frac{\phi c_t \mu}{k}\frac{\partial p}{\partial t} \qquad (1)$$

with p pressure in the borehole

c_t compressibility

r distance to the borehole axis

k permeability

ϕ porosity

μ viscosity.

The pressure can be solved analytically as function of distance r and time t:

$$p_D = \frac{8\alpha}{\pi^2} \int_0^\infty \frac{\exp\left(\frac{-\beta u^2}{\alpha}\right)}{u\left[\left(uJ_0(u) - 2\alpha J_1(u)\right)^2 + \left(uY_0(u) - 2\alpha Y_1(u)\right)^2\right]} du \qquad (2)$$

with $\beta = \frac{kht\pi}{V_w c_t \mu}$ and $\alpha = \frac{\pi r_w^2 \phi c_t h}{V_w c_t}$

and J_0 Bessel function first type order null

J_1 Bessel function first type first order

Y_0 Weber function order null

Y_1 Weber function first order

c_t compressibility

h length of the tested borehole interval

r_w borehole radius

V_w fluid volume in the tested borehole interval.

The solution for the diffusivity equation was introduced by COOPER et al. (1967) for an open borehole and BREDEHOEFT & PAPADOPULOS (1980) transferred this solution to a closed borehole. Opposite to the notation of the cited authors instead of the head difference as function of storage capacity and transmissibility in equation 2 the dimensionless pressure as function of porosity and permeability is used in the following. The dimensionless pressure p_D can be converted into the pressure in the borehole using the following equation:

$$p_D = \frac{p_i - p_w}{p_i - p_0} \qquad (3)$$

with p_D dimensionless pressure

p_i initial formation pressure

p_0 initial pressure in the borehole

p_w pressure in the borehole at the considered point in time

With equation 2 and 3 the necessary equations to calculate the pressure evolution for a pulse test are available. Pressure evolutions for different permeabilities were calculated with these equations and then compared to a measured pressure evolution. The permeability of the rock is found when measured and calculated pressure evolutions agree well.

In equation 2 there is beneath the permeability the porosity as a parameter that is not determined by the boundary conditions of the test. Permeability and porosity affect the pressure evolution in different ways, compare Figure 4-6.

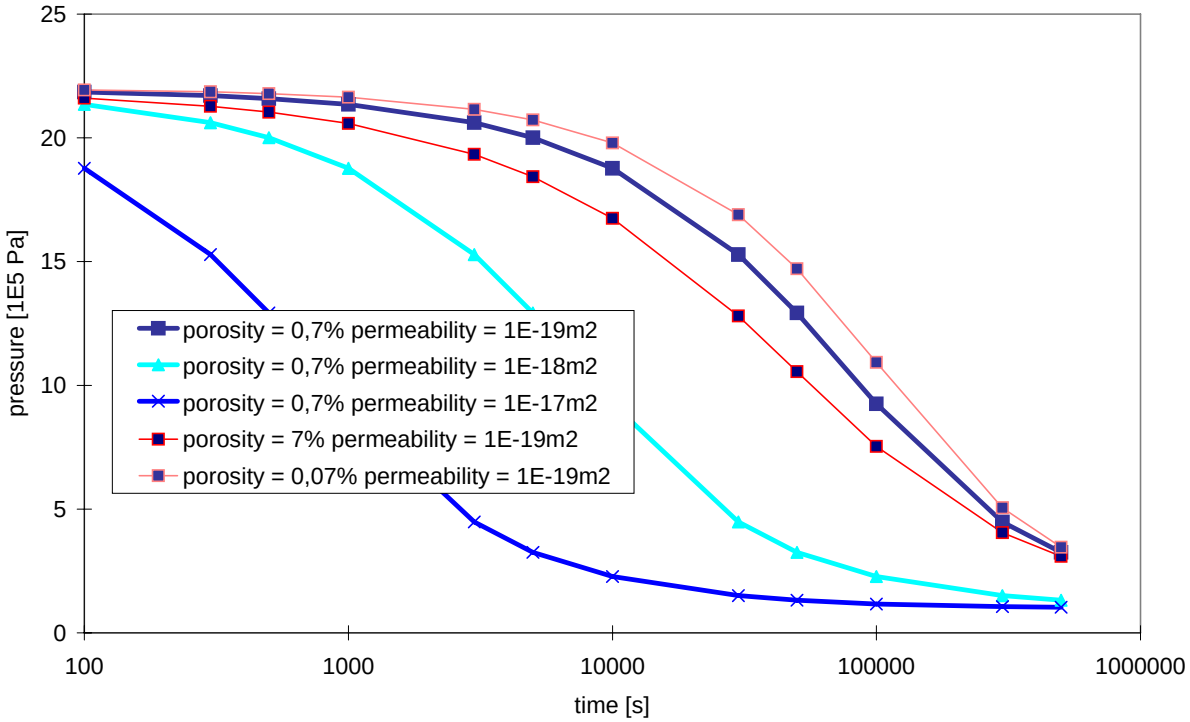

Figure 4-6. *Effect of porosity and permeability on the pressure evolution in a pulse test.*

Figure 4-6 shows the influence of different values of porosity and permeability on the pressure evolution in a virtual pulse test. Porosity has an influence on the *shape* of the pressure evolution (red curves). Alteration of permeability leads to a *shift* of the pressure evolution with respect to the (logarithmic) time axis without alteration of the shape. For this reason the determination of permeability from a pulse test is hardly influenced by the porosity.

For interpretation of the results from that method it is important to notice that the gained value is not the intrinsic permeability of the rock; two-phase flow has to be considered.

5 Measurements

5.1 Deposition Hole DA3147G01 (LASGIT)

On the position without visible fractures (compare Figure 2-4) a test sequence of two pulses ($1.6 \cdot 10^5$ Pa and $2.2 \cdot 10^5$ Pa) was conducted. An axially symmetric model was used for the test analysis (compare chapter 4.1). It is assumed that the granite in the tested area is initially water saturated. With seawater as test fluid two-phase-flow phenomena can be neglected.

The initial water pressure in the rock was assumed to be equal to the measured gas pressure in the deposition hole (105900 Pa), the initial pressure in the test volume of the surface packer corresponds to the first pressure pulse of $1.6 \cdot 10^5$ Pa. At the second pressure pulse the calculation was restarted with the calculated pressure distribution in the rock at that time and $2.2 \cdot 10^5$ Pa in the test volume of the surface packer system. The measured gas pressure in the deposition hole was used as boundary condition; all other boundaries of the model were closed.

Figure 5-1 shows a comparison of the measured pressure evolution in the surface packer (grey line) and calculated pressure evolutions for several permeabilities (parameter values are in m^2). At the end of the first pressure pulse the measured pressure was $1.59 \cdot 10^5$ Pa. If the rock had a permeability of only 10^{-20} m² the pressure should have been higher, according to the results of the numerical model about $1.65 \cdot 10^5$ Pa. If the rock had a permeability of $3 \cdot 10^{-19}$ m² the pressure should have been lower, according to the results of the numerical model below $1.5 \cdot 10^5$ Pa. From Figure 5-1 it becomes clear that a minimum test duration is necessary to differentiate the pressure evolutions for certain permeability values. The calculated pressure evolution for a permeability of the rock of 10^{-19} m² agrees well with the measured data.

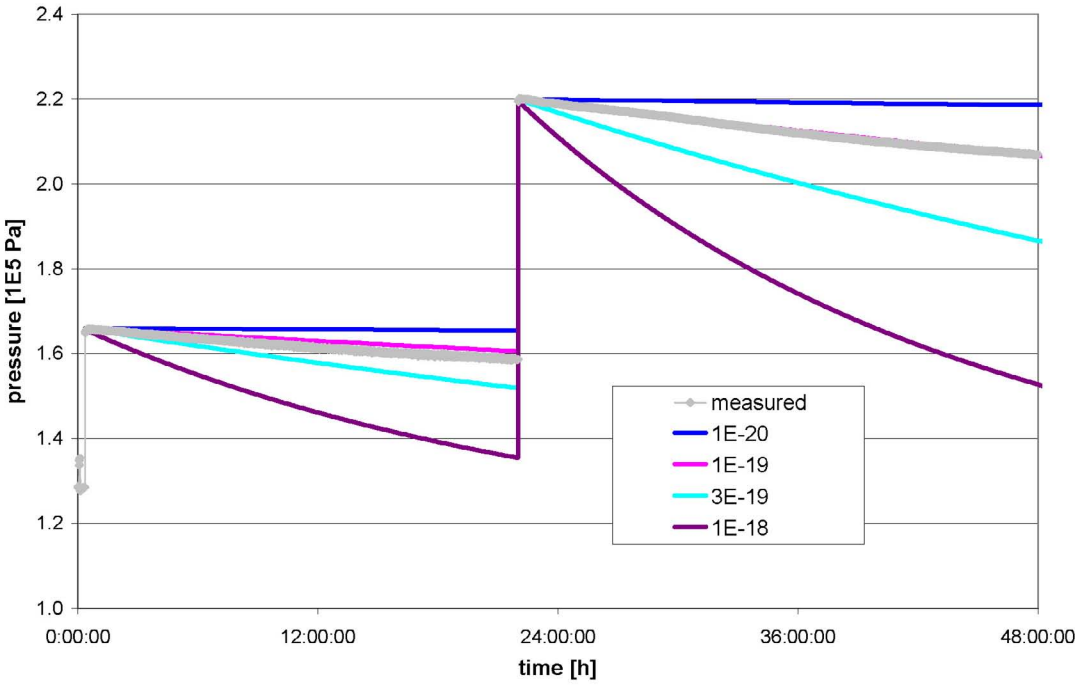

Figure 5-1. *Result from surface packer test in deposition hole DA3147G01 (LASGIT).*

5.2 Q-Tunnel

For the test locations in the Q-tunnel refer to chapter 2.2. An axially symmetric model with adopted initial and boundary conditions was used for the test analysis (compare chapter 4.1).

Figure 5-2 shows a comparison of the measured pressure evolution in the surface packer (grey line with symbols) and calculated pressure evolutions for several permeabilities (parameter values are in m^2). Derivatives for all these curves are plotted also to provide an additional criterion for the test analysis. For test no. 1 the sudden decrease of pressure in the measured data at early time was not caused by flow of water into the rock; it was an artefact from the test equipment. The best agreement between calculated pressure evolution/derivative and measured data/derivative is for a permeability of the rock smaller $8 \cdot 10^{-20}$ m^2. For test no. 2 the best agreement is for a permeability of the rock $5 \cdot 10^{-20}$ m^2, for test no. 3 between 10^{-19} m^2 and $3 \cdot 10^{-19}$ m^2, and for test no. 4 the value is $5 \cdot 10^{-19}$ m^2. The diagrams include in the header the name of the raw data files in the SICADA database.

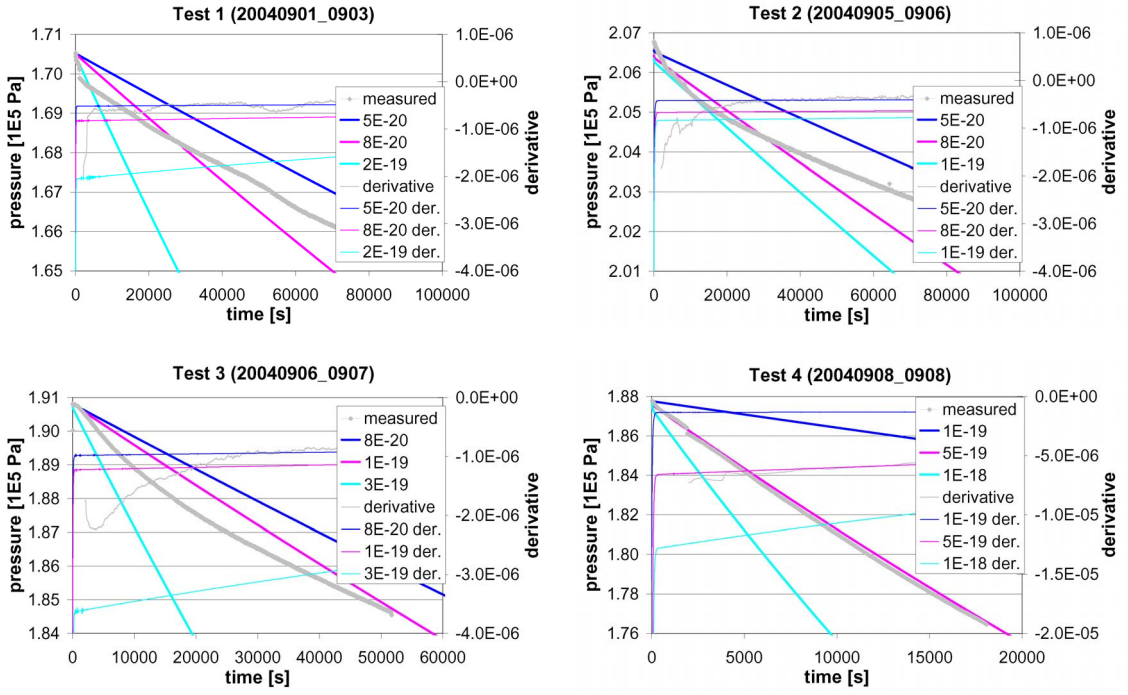

Figure 5-2. *Result from tests in the Q-tunnel.*

For the interpretation of this result the typical star-shaped pattern of cracks around a blast hole has to be considered (compare Figure 2-2). The parameter values derived from these tests are not valid for the cracks.

5.3 A-Tunnel

For the investigation of the excavation damaged zone in a gallery excavated by TBM BGR performed test in the A-tunnel with gas, with water, and with Helium.

5.3.1 Tests with Gas

In the first test test series hydraulic tests with gas were performed. Tests with the surface packer / mini packer system are small scale interference tests: while a pressure pulse is applied to the surface packer also the pressure response in the central borehole is monitored (and vice versa). Two-phase-flow conditions had to be considered for the analysis of the tests.

Pressure pulses were varied between 0.5 MPa and 1 MPa. Except for one test at PA3474A01 all of these tests had in common that no connection between the borehole and the area beneath the surface packer was observed, even though the shortest distance between these test volumes was 3.5 cm (which is the length of the mini packer).

Figure 5-3 shows the evolution of pressure vs. time (logarithmic scale) for the tests with about 0.5 MPa pressure pulses in the borehole mini packer (left) and in the surface packer (right). At one location the tests were conducted with 0.8 MPa (Figure 5-4) and 1 MPa (Figure 5-5). The pressure evolutions are normalized to ease comparison:

$$p_n = (p_t - 0.1\ \text{MPa}) / (p_i - 0.1\ \text{MPa})$$

p_n normalized pulse pressure [-]

p_t pressure at time t

p_i initial pulse pressure

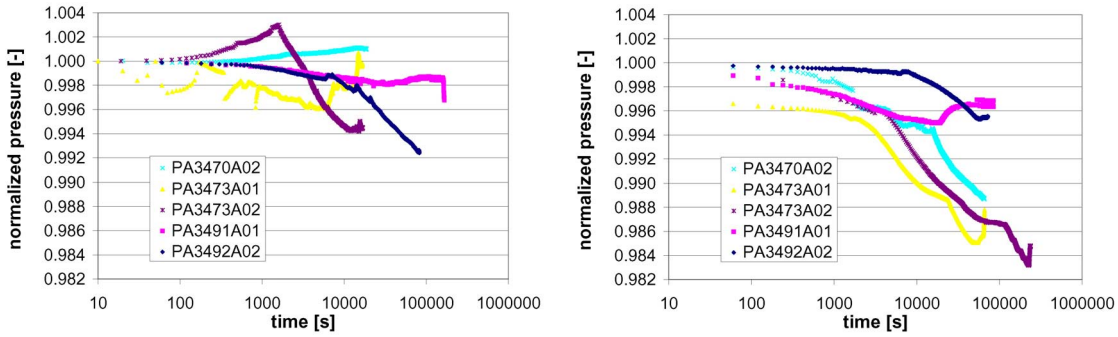

Figure 5-3. *Result from tests with gas in the A-tunnel, 0.5 MPa pulse pressure: borehole (left) and surface packer (right).*

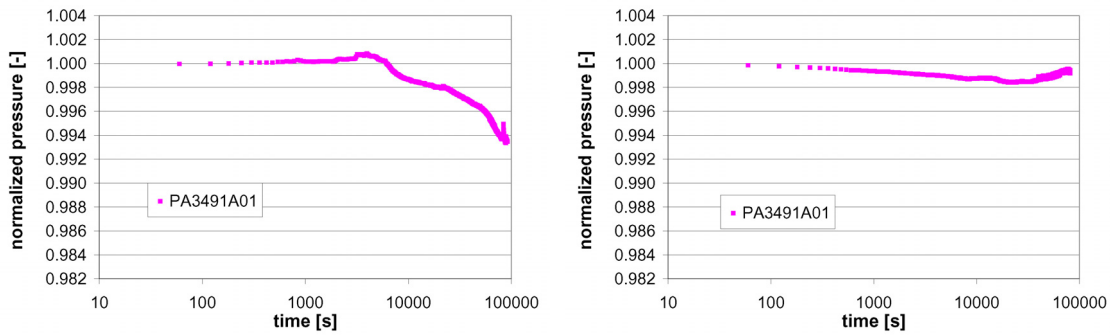

Figure 5-4. *Result from tests with gas in the A-tunnel, 0.8 MPa pulse pressure: borehole (left) and surface packer (right).*

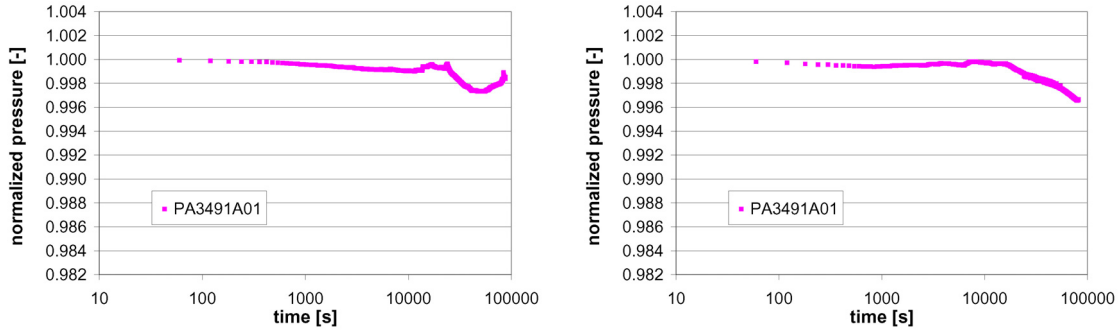

Figure 5-5. *Result from tests with gas in the A-tunnel, 1.0 MPa pulse pressure: borehole (left) and surface packer (right).*

All tests showed no clear pressure reduction. Basing on the theory of two-phase flow these tests can be interpreted such that the gas entry pressure at these locations was not exceeded by the pressure pulses of up to 1 MPa during the tests.

At PA3474A01 one exception was found. The test sequence started with a pulse of about 1 MPa (phase 1) in the borehole mini packer (Figure 5-6). After about half day the pressure in the borehole began to decrease while in the surface packer a pressure increase was monitored. After this test the sequence was continued with phase 2, a pulse in the surface packer (after pressure release in both packers). From the start of the phase 2 a response in the borehole was monitored. At two points in time a sudden acceleration of pressure build-up in the borehole was monitored.

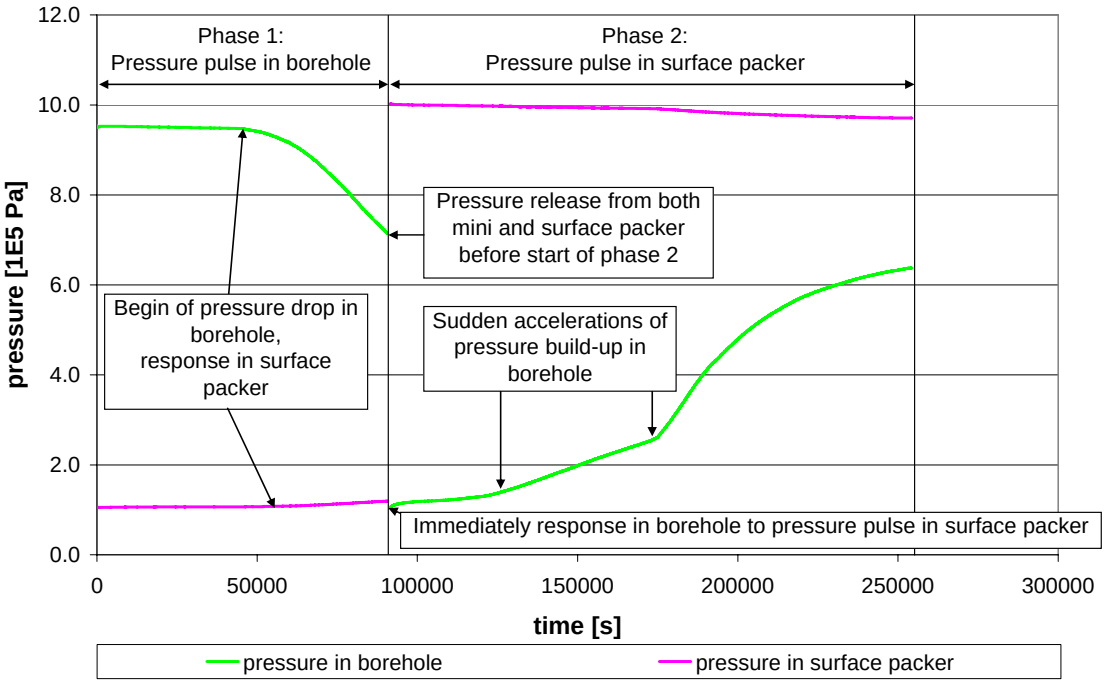

Figure 5-6. *Result from tests with gas in the A-tunnel, location PA3474A01.*

Basing on the theory of two-phase flow this test can be interpreted such that a gas-filled pathway through the (partially) water saturated pore space between borehole and surface was formed during test phase 1; this observation would not had been made if the test was stopped before. The immediate response of pressure in the borehole after the pulse in the surface packer in phase 2 indicates that this pathway still existed after the pressure release in both packers. The two sudden accelerations of pressure build up during phase 2 indicate the formation of new pathways between borehole and surface, most probable due to water displacement.

5.3.2 Tests with Water

In the second test test series hydraulic tests with water were performed. The tests were performed on the same positions as the tests with gas, but for technical reasons without the mini packer.

Figure 5-7 shows the measured pressure evolutions in the surface packer (black line with symbols) and their derivatives (grey line). The calculated evolutions of pressure for permeability values of 10^{-21} (blue), $5 \cdot 10^{-21}$ (magenta), 10^{-20} (light blue), and $5 \cdot 10^{-20}$ m^2 (orange) are in the same plot with a thick line, the corresponding derivatives are in the same colour with a thin line.

The first of these tests had been performed on location PA3473A01. Execution and analysis of this test are described more in detail; for the rest of the tests only the results are presented in Table 5-1. In this test the initial pressure was $4.53 \cdot 10^5$ Pa. At the end of the test after 83940 s (about 1 day) the pressure was still at $4.03 \cdot 10^5$ Pa.

Then pressure was released from the testing volume (surface packer and pressure vessel, compare Figure 3-5) down to the pressure of $1.07 \cdot 10^5$ Pa in the gallery via the air escape valve. Like in all other tests a bubble-free jet of water came from the valve, in total about 42 cm^3. The equipment had been filled with water very carefully, so it can be assumed that this water outflow is caused by the expansion of the inevitable volume of gas trapped in the equipment (compare Figure 4-1). So there are 42 cm^3 of air (at $1.07 \cdot 10^5$ Pa) in the equipment, which had a volume of about 10 cm^3 at the initial pulse pressure ($4.53 \cdot 10^5$ Pa). This volume corresponds to a “gas saturation” of about 1% for the complete testing volume (compare Table 3-2). The gas saturated volume in the model had been adjusted to that value to reproduce the total compressibility of the two phases in the testing volume; nevertheless the fluid going into the rock is just the aqueous phase. In the test on location PA3473A02 only 15 cm^3 of water were collected when pressure was released from the testing volume. That means that the total compressibility of the fluids (inevitable trapped air and water) in the testing volume was significant lower than in the test on location PA3473A01. The effect of different total compressibility can be seen in Figure 5-7 by comparing for these two tests the calculated pressure evolution for a permeability of $5 \cdot 10^{-20}$ m^2: in the case of lower total compressibility (PA3473A02) the calculated pressure drop is more pronounced than in the case of higher total compressibility (PA3473A01).

At the end of the test the measured pressure was $4.03 \cdot 10^5$ Pa. If the rock had a permeability of only 10^{-21} m^2 the pressure should have been higher, according to the results of the numerical model more than $4.3 \cdot 10^5$ Pa. If the rock had a permeability of $5 \cdot 10^{-21}$ m^2 the pressure should have been lower, according to the results of the numerical model clearly less than $4 \cdot 10^5$ Pa. This means the permeability at location PA3473A01 is smaller than $5 \cdot 10^{-21}$ m^2 (in direction of measurement).

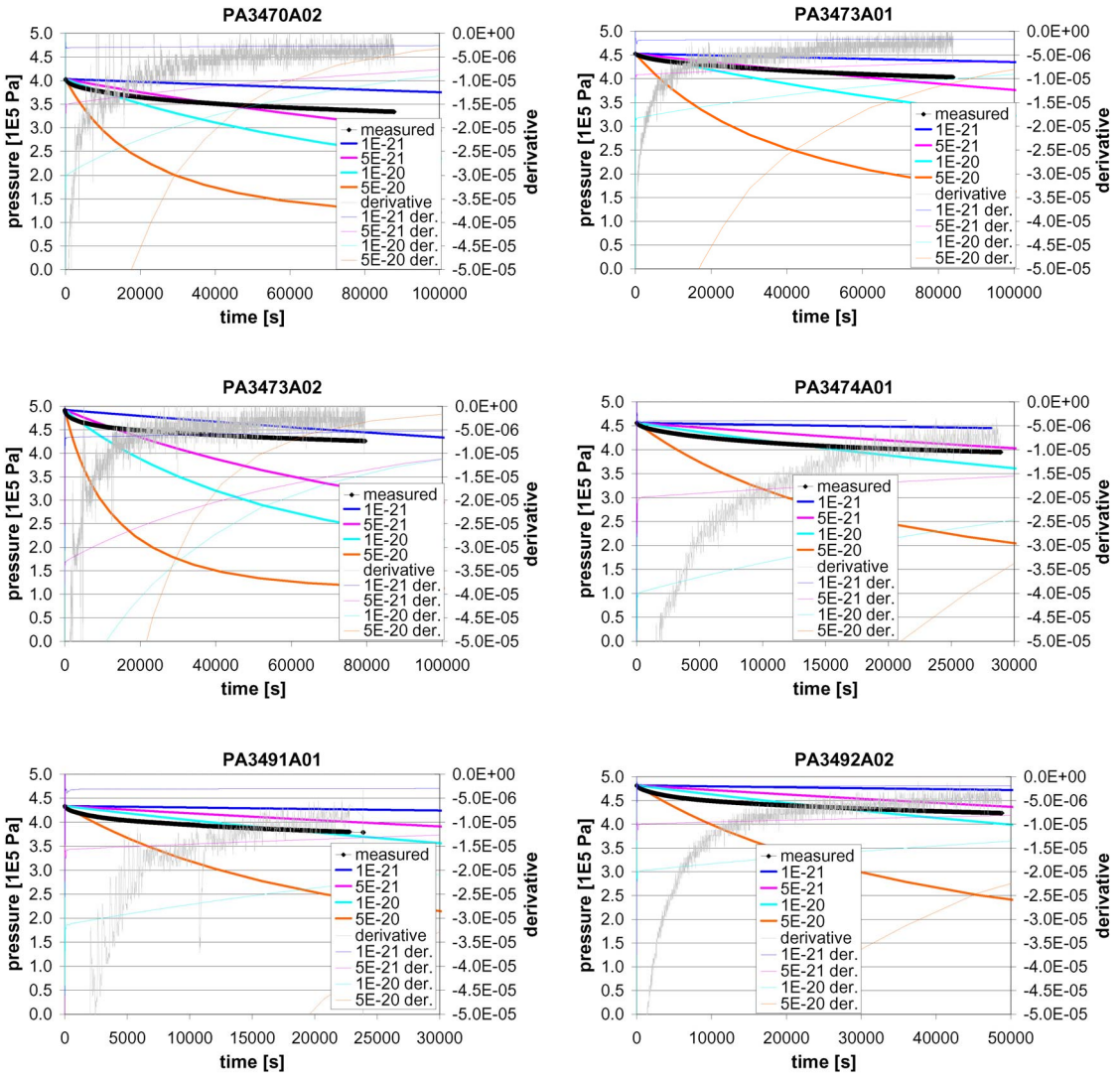

Figure 5-7. *Results from tests with water in the A-tunnel: Diagrams.*

Table 5-1. Results from tests with water in the A-tunnel: permeability values.

location	permeability [m^2]
PA3470A02	$< 5 \cdot 10^{-21}$
PA3473A02	$< 5 \cdot 10^{-21}$
PA3473A01	$< 5 \cdot 10^{-21}$
PA3474A01	$< 1 \cdot 10^{-20}$
PA3491A01	$< 1 \cdot 10^{-20}$
PA3492A02	$< 1 \cdot 10^{-20}$

5.3.3 Tests with Helium

In the third test series two locations were tested with Helium with the surface packer / mini packer equipment.

The test on location PA3474A01 was performed as a sequence of two pressure pulses in the central borehole (compare chapter 3, Figure 3-6). After the first pressure pulse of $3.05 \cdot 10^5$ Pa a quick drop in pressure (down to about the pressure value in the gallery) was monitored in the borehole. A second pressure pulse of $4.1 \cdot 10^5$ Pa was initiated after 45 hours without making any changes of the equipment installation. For the second pressure pulse a slow drop in pressure was monitored. Figure 5-8 shows the measured pressure evolution in the borehole for the complete test (black symbols) and the volumetric Helium concentration of the gas flow into the sensor hose line (red symbols). The points in time where the Helium detector was maintained are marked with vertical dashed red lines. The measured temperature remained about constant during the test (17.5 ± 0.5 °C).

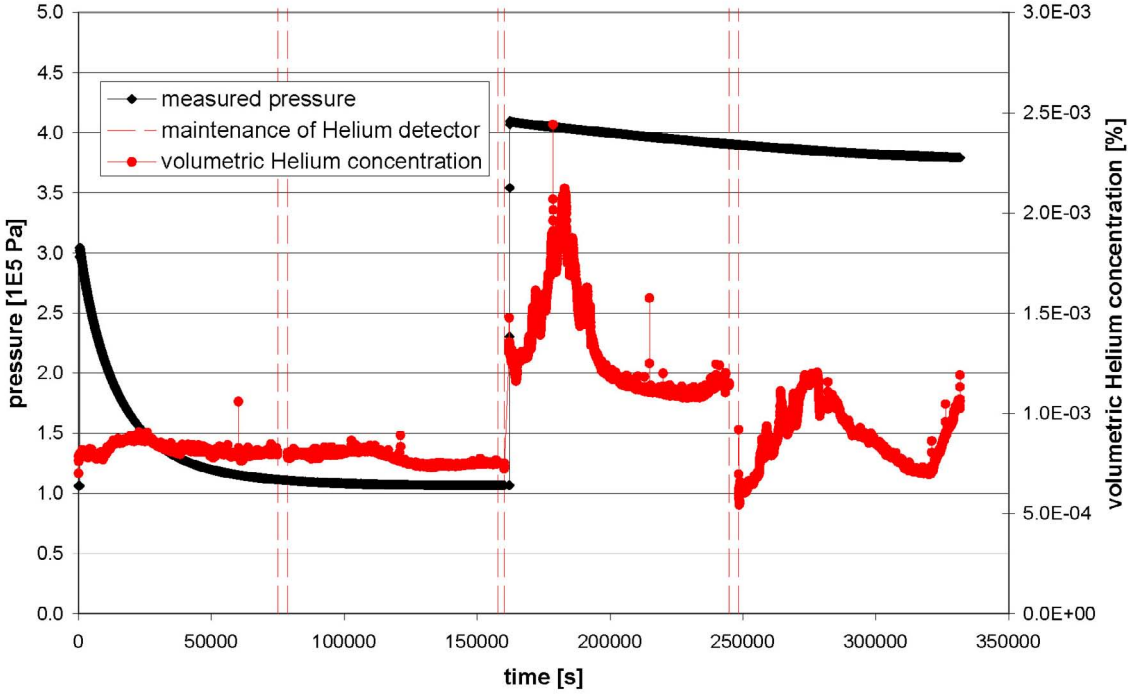

Figure 5-8. *Pressure evolution in borehole and volumetric Helium concentration for tracer test on PA3474A0.1*

Additionally Figure 5-9 shows the volumetric Helium concentration of the gas flow into the sensor hose line (red symbols) in comparison to the measured pressure in the gallery.

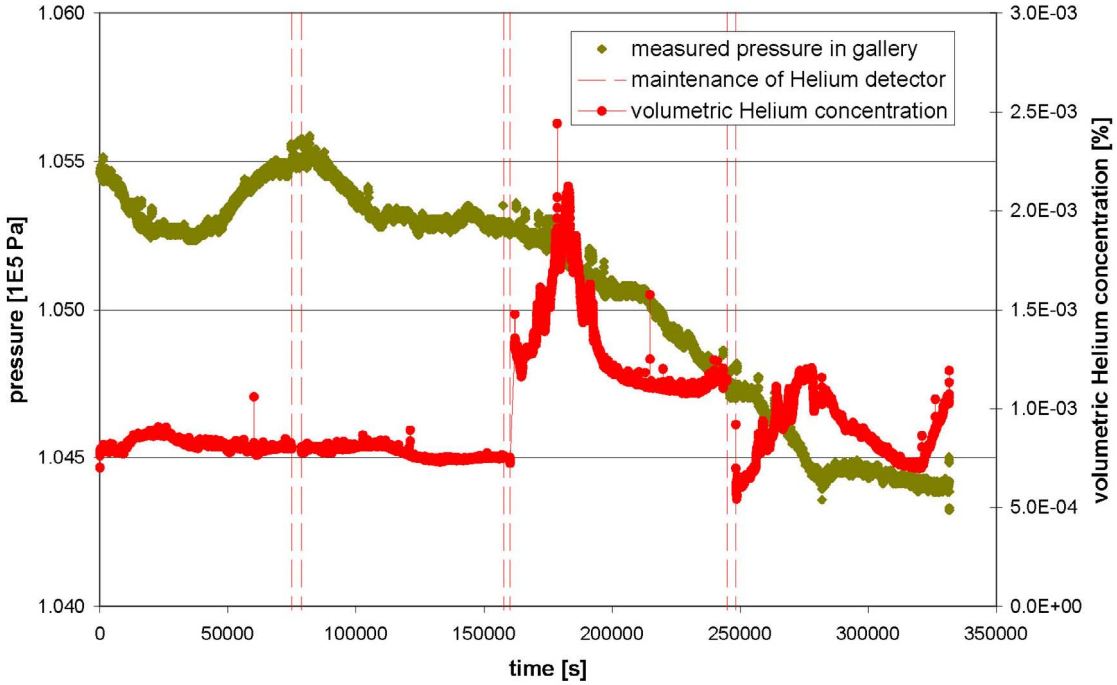

Figure 5-9. *Pressure evolution in gallery and volumetric Helium concentration for tracer test on PA3474A01.*

The test on location PA3473A01 was performed with a pressure pulse of $4.13 \cdot 10^5$ Pa. A slow drop in pressure was monitored. Figure 5-10 shows the measured pressure evolution and the volumetric Helium concentration of the gas flow into the sensor hose line. The points in time where the Helium detector was maintained are marked with vertical dashed red lines. The measured temperature remained at 18.2 ± 0.4 °C.

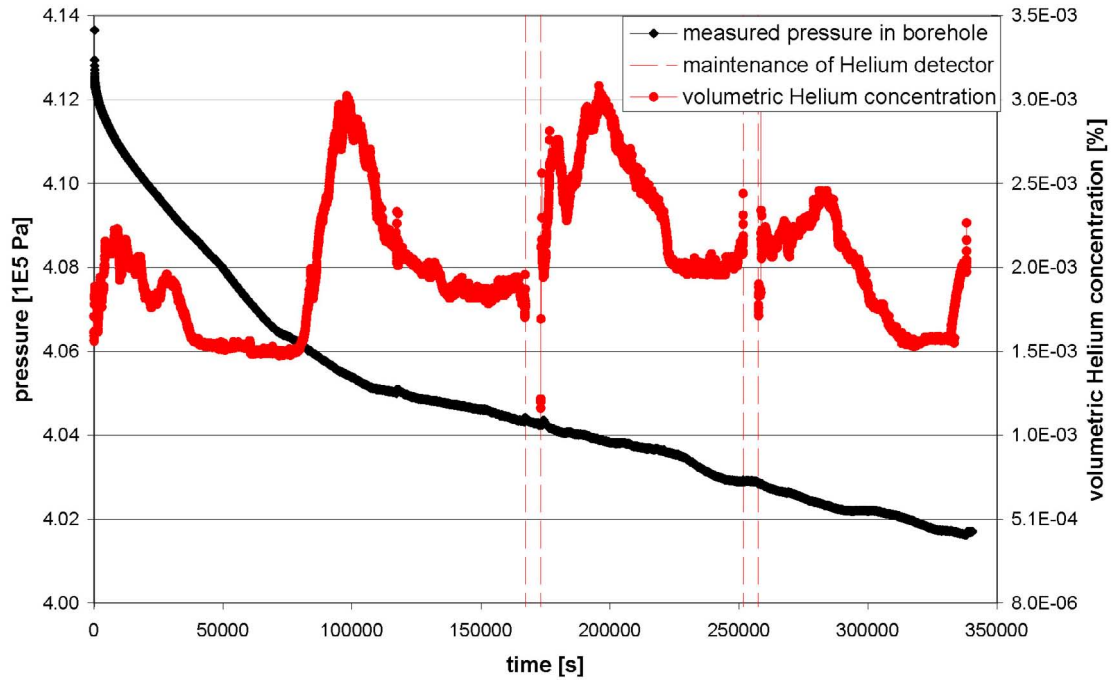

Figure 5-10. *Pressure evolution in borehole and volumetric Helium concentration for tracer test on PA3473A01.*

Additionally Figure 5-11 shows the volumetric Helium concentration of the gas flow into the sensor hose line (red symbols) in comparison to the measured pressure in the gallery.

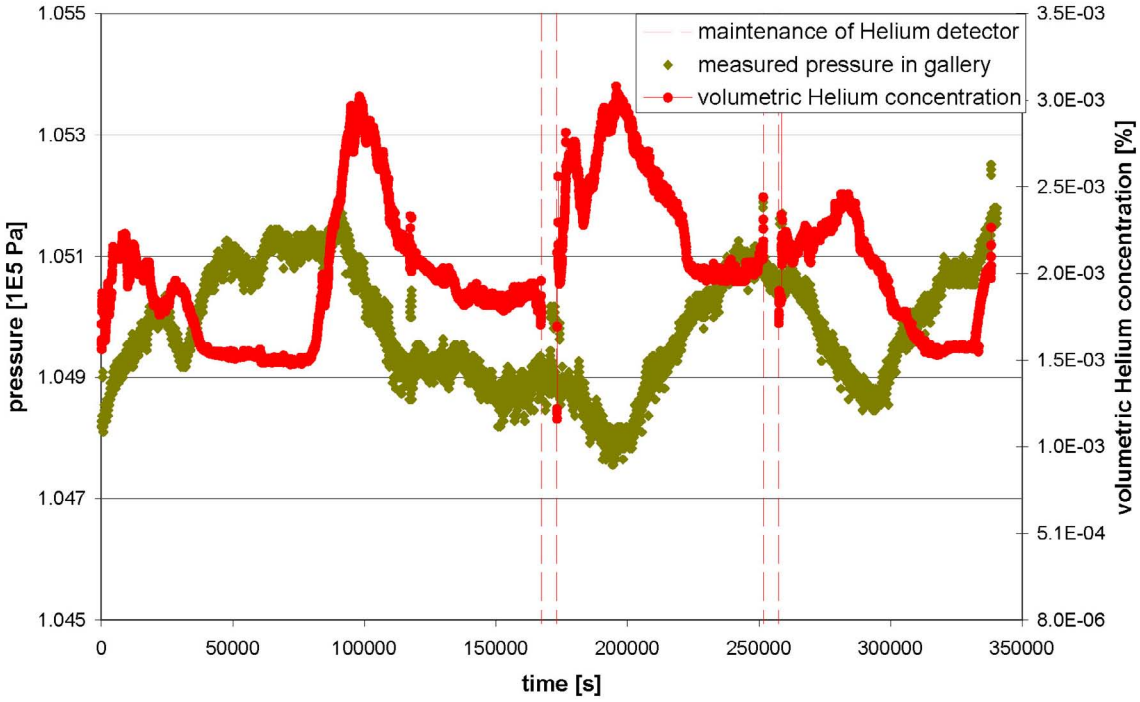

Figure 5-11. *Pressure evolution in gallery and volumetric Helium concentration for tracer test on PA3473A01.*

Results with respect to permeability

Beneath the analysis as tracer test the measured pressure evolutions in the borehole have been analyzed with an analytical method for one-phase flow as pulse tests; the method is described in chapter 4.3. For interpretation of the results from that method it is important to notice that the gained value is not the intrinsic permeability of the rock; two-phase flow has to be considered.

For the test analysis the porosity of the rock has been set with 0.2 %. The permeability has been varied in the calculation; the permeability value is obtained by comparison of measured pressure evolution with calculated pressure evolution.

For the test on location PA3474A01 Figure 5-12 shows this comparison for the first pressure pulse and Figure 5-13 for the second pressure pulse.

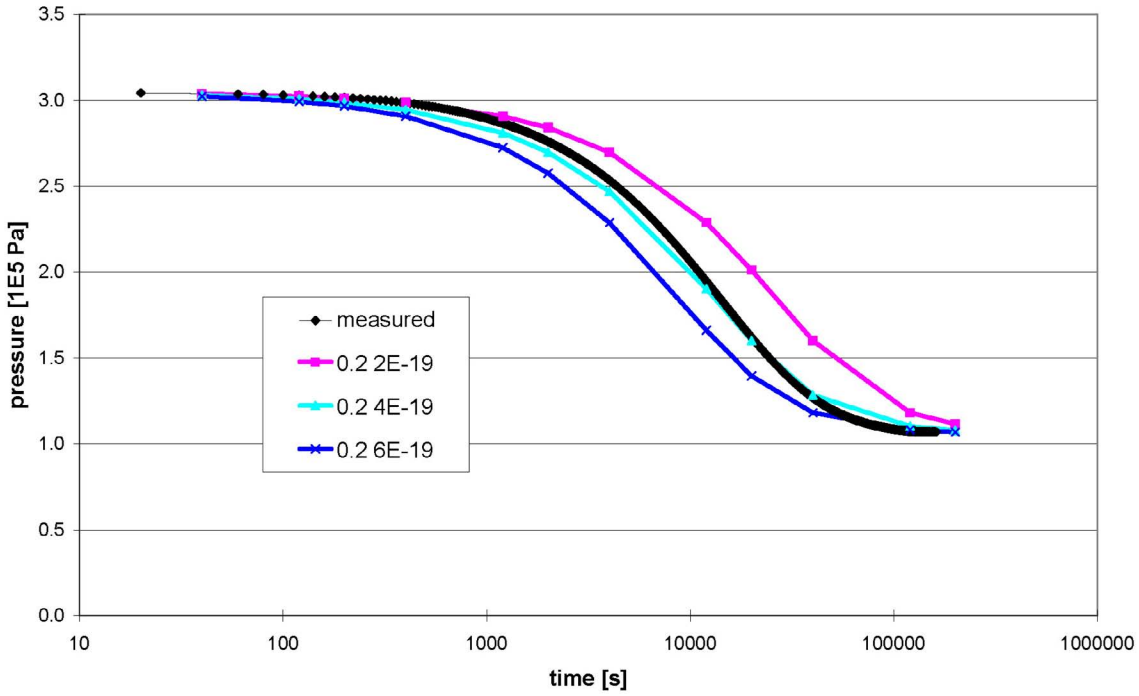

Figure 5-12. *Result of first pressure pulse on PA3474A01 with respect to Helium permeability.*

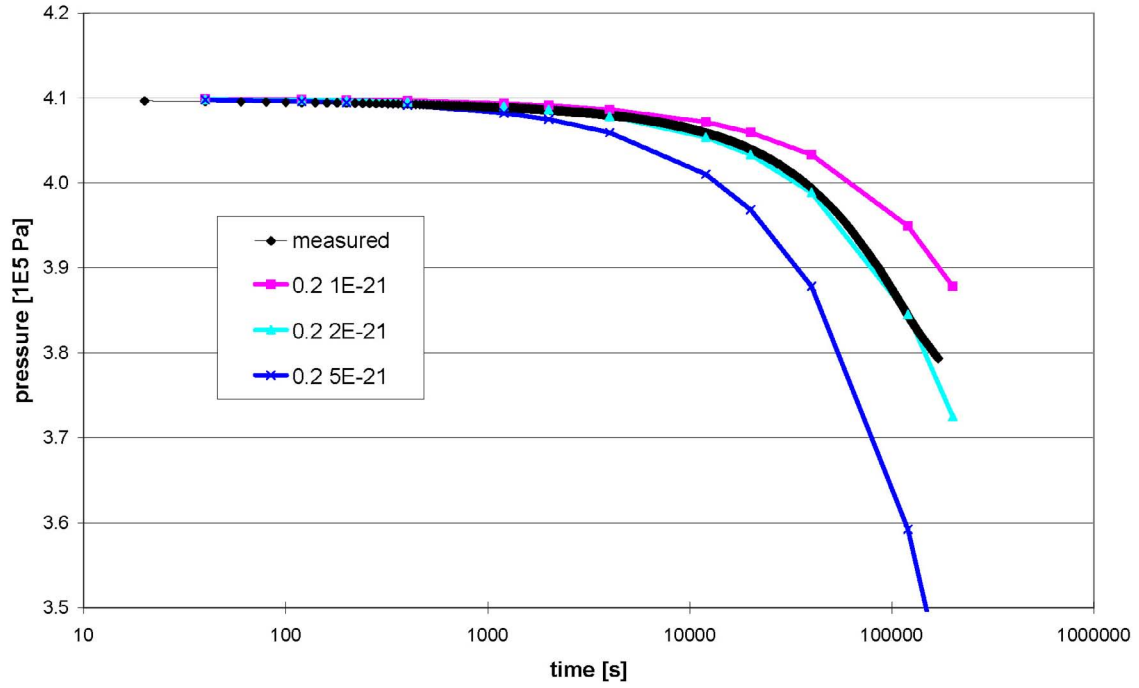

Figure 5-13. *Result of second pressure pulse on PA3474A01 with respect to Helium permeability.*

After 12000 s the measured pressure was $1.95 \cdot 10^5$ Pa for the first pressure pulse. If the rock had a Helium permeability ($k_{rg}\mathbf{k}$, constant value) of $2 \cdot 10^{-19}$ m^2 the pressure should have been higher, according to the analytical method $2.29 \cdot 10^5$ Pa. If the rock had a Helium permeability ($k_{rg}\mathbf{k}$, constant value) of $4 \cdot 10^{-19}$ m^2 the pressure should have been little lower, according to the analytical method $1.9 \cdot 10^5$ Pa. The second pressure pulse was initiated after the pressure in the borehole had fallen down to about the value in the gallery. Though no changes of the equipment installation had been made the result was very different. After 120000 s the measured pressure was $3.84 \cdot 10^5$ Pa. If the rock had a Helium permeability ($k_{rg}\mathbf{k}$, constant value) of 10^{-21} m^2 the pressure should have been higher, according to the analytical method $3.95 \cdot 10^5$ Pa. If the rock had a Helium permeability ($k_{rg}\mathbf{k}$, constant value) of $5 \cdot 10^{-21}$ m^2 the pressure should have been lower, according to the analytical method $3.59 \cdot 10^5$ Pa.

For the test on location PA3473A01 Figure 5-14 shows the measured and calculated pressure evolutions.

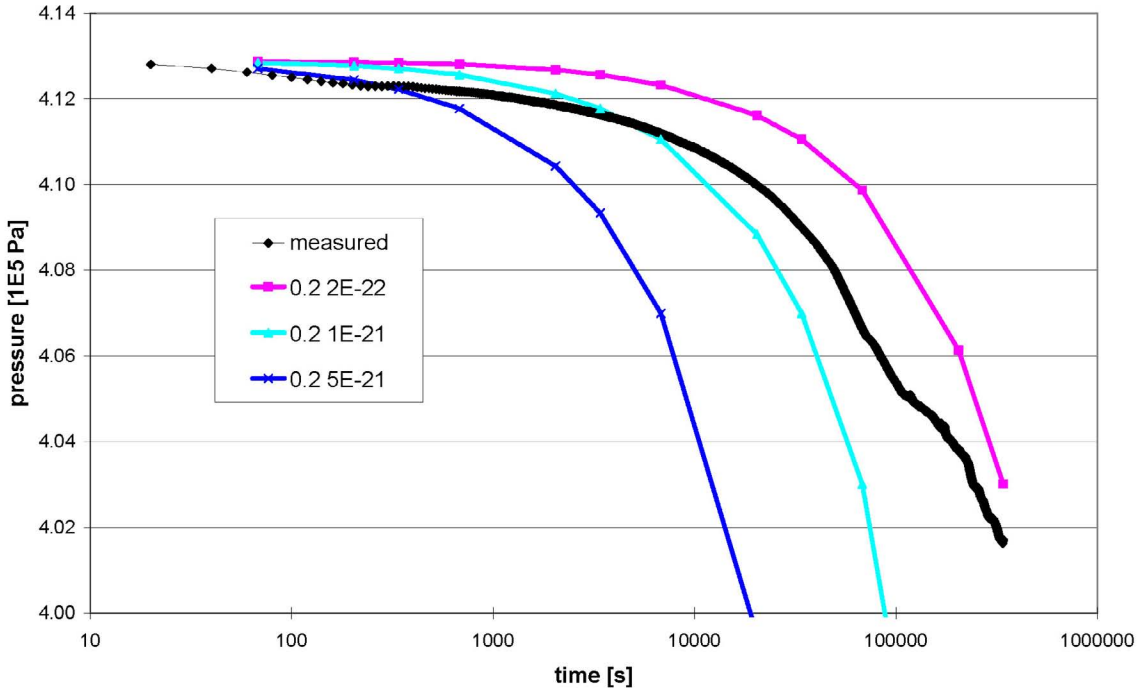

Figure 5-14. *Result of pressure pulse on PA3473A01 with respect to Helium permeability.*

After 340000 s (about the end of the test) the measured pressure was $4.02 \cdot 10^5$ Pa. If the rock had a Helium permeability ($k_{rg}\mathbf{k}$, constant value) of $2 \cdot 10^{-22}$ m^2 the pressure should have been little higher, according to the analytical method $4.03 \cdot 10^5$ Pa. If the rock had a Helium permeability ($k_{rg}\mathbf{k}$, constant value) of $1 \cdot 10^{-21}$ m^2 the pressure should have been lower, according to the analytical method $3.79 \cdot 10^5$ Pa.

In combination with the measured permeabilities with water (compare chapter 5.3.2) and an assumption to the course of the two-phase flow parameters capillary pressure and relative permeabilities for water and gas the initial saturation with gas can be estimated (compare chapter 4.2, Figure 4-4). The parameters from UPC give a higher gas entry pressure which corresponds to the observations that had been made in the hydraulic tests with the surface packer / mini packer combination with gas as test medium (compare chapter 5.3.1), therefore the data set from UPC was used in the following test analysis.

The surface packer test on location PA3474A01 with water as test medium (compare Table 5-1) gave no evidence for hydraulic properties that differ significantly from the other tested locations. The permeability value is in the range $5 \cdot 10^{-21}$ m^2 to 10^{-20} m^2, chosen value for the analysis of the tracer tests is $7 \cdot 10^{-21}$ m^2. Taking the coarse estimation for $k_{rg}\mathbf{k}$ for the first pressure pulse from the analytical method ($2 \cdot 10^{-19}$ m^2 to $4 \cdot 10^{-19}$ m^2) the value for k_{rg} is about 43 and thereby out of range for the classical definition of two-phase flow parameters. Taking the coarse estimation for $k_{rg}\mathbf{k}$ for the second pressure pulse from the analytical method (10^{-21} m^2 to $5 \cdot 10^{-21}$ m^2, value chosen with $2 \cdot 10^{-21}$ m^2) the value for k_{rg} is 0.29. Assuming $k_{rg} + k_{rw} = 1$ and rearranging the UPC-relation for relative water permeability this yields in a value for water saturation of 97.5% which is a reasonable value.

The surface packer test on location PA3473A01 with water as test medium (compare Table 5-1) gave a permeability value in the range 10^{-21} m^2 to $5 \cdot 10^{-21}$ m^2, chosen value for the analysis of the tracer tests is $3 \cdot 10^{-21}$ m^2. Taking the coarse estimation for $k_{rg}\mathbf{k}$ from the analytical method ($2 \cdot 10^{-22}$ m^2 to 10^{-21} m^2, value chosen with $2 \cdot 10^{-22}$ m^2 as it fits best the end of the test) the value for k_{rg} is 0.07. This yields in a value for water saturation of 99.8% which is (also) a reasonable value.

Results with respect to transport properties

The analysis of the measured data had been started with the test on location PA3473A01.

The initial Helium volume concentration in the gas phase within the rock volume was set according to the measured volumetric Helium concentration of the gas flow into the sensor hose line before the pressure pulse was initiated: $6.951 \cdot 10^{-6}$ m^3/m^3 for the (foregoing) test on PA3474A01 and $1.785 \cdot 10^{-5}$ m³/m³ for the test on PA3473A01 (this second, slightly increased value might already had been influenced by the previous test on PA3474A01).

Figure 5-15 shows the measured and calculated evolutions of pressure in the borehole and volumetric Helium content of the gas flow into the sensor hose line. The diffusion coefficient in the calculation was 10^{-7} m^2/s. The bold lines are for pressure, the thin lines are for volumetric Helium content. The light blue lines are for the permeability value as described in the foregoing chapter, $3 \cdot 10^{-21}$ m^2. Additionally there are plots for permeability values one order of magnitude lower ($3 \cdot 10^{-22}$ m^2, dark blue lines) and one order of magnitude higher ($3 \cdot 10^{-20}$ m^2, orange lines). The pink lines are for a permeability value of 10^{-21} m^2.

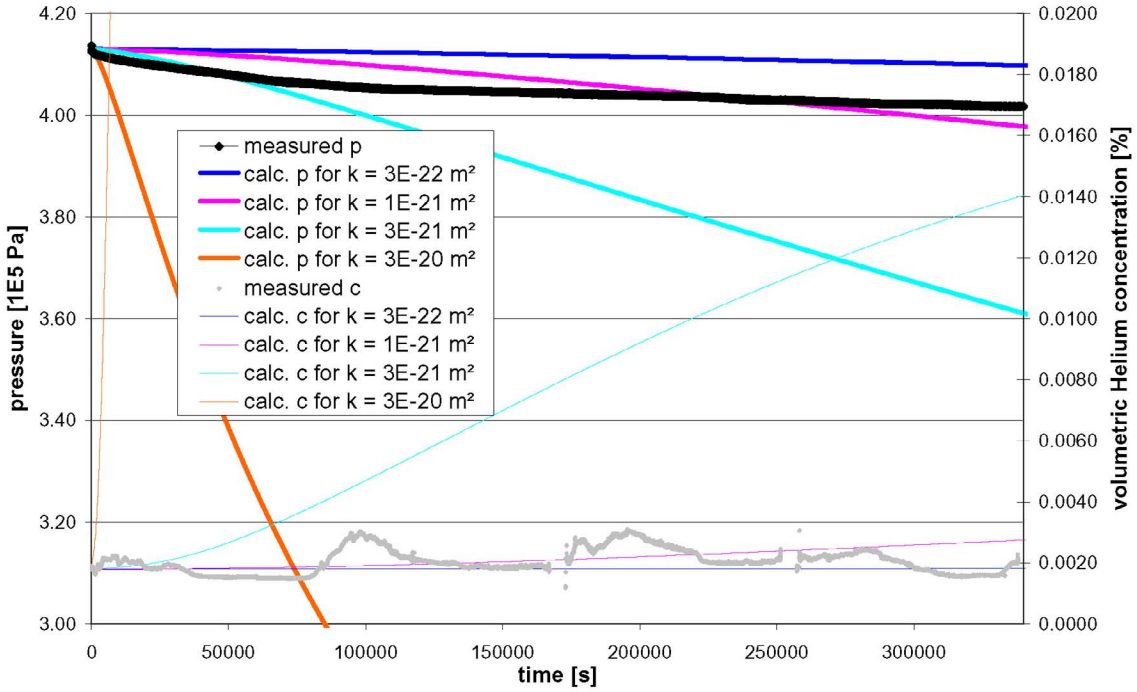

Figure 5-15. *Results for tracer test on PA3473A01: variation of permeability.*

Neither for the pressure evolution nor the evolution of volumetric Helium content of the gas flow into the sensor hose line measured and calculated data agree for the permeability value of $3 \cdot 10^{-21}$ m^2. At the end of this test the measured pressure was $4.02 \cdot 10^5$ Pa. If the rock had a permeability of $3 \cdot 10^{-21}$ m^2 (and the two-phase flow parameters are appropriate, compare Figure 4-4) the pressure should have been lower, according to the results of the numerical model $3.58 \cdot 10^5$ Pa; the even more pronounced disagreement for the permeability value of $3 \cdot 10^{-20}$ m^2 is obvious. The best agreement of measured and calculated data is for the permeability of 10^{-21} m^2 (with the chosen two-phase flow parameters) not only for the pressure evolution but also for the evolution of volumetric Helium content of the gas flow into the sensor hose line. The calculation with a permeability value of $3 \cdot 10^{-22}$ m^2 (with the chosen two-phase flow parameters) results in a drop of pressure that is too small in comparison to the measured data and also this calculation can not explain that Helium was found by the detector.

Figure 5-16 shows the influence of diffusion coefficient. The permeability value in the calculations for that comparison was 10^{-21} m^2. The bold pink line is for pressure. The thin pink line is for a diffusion coefficient of 10^{-7} m^2/s, the thin orange line is for a diffusion coefficient of $1.8 \cdot 10^{-6}$ m^2/s. These calculations gave no significant difference for the volumetric Helium content of the gas flow into the sensor hose line for this test configuration.

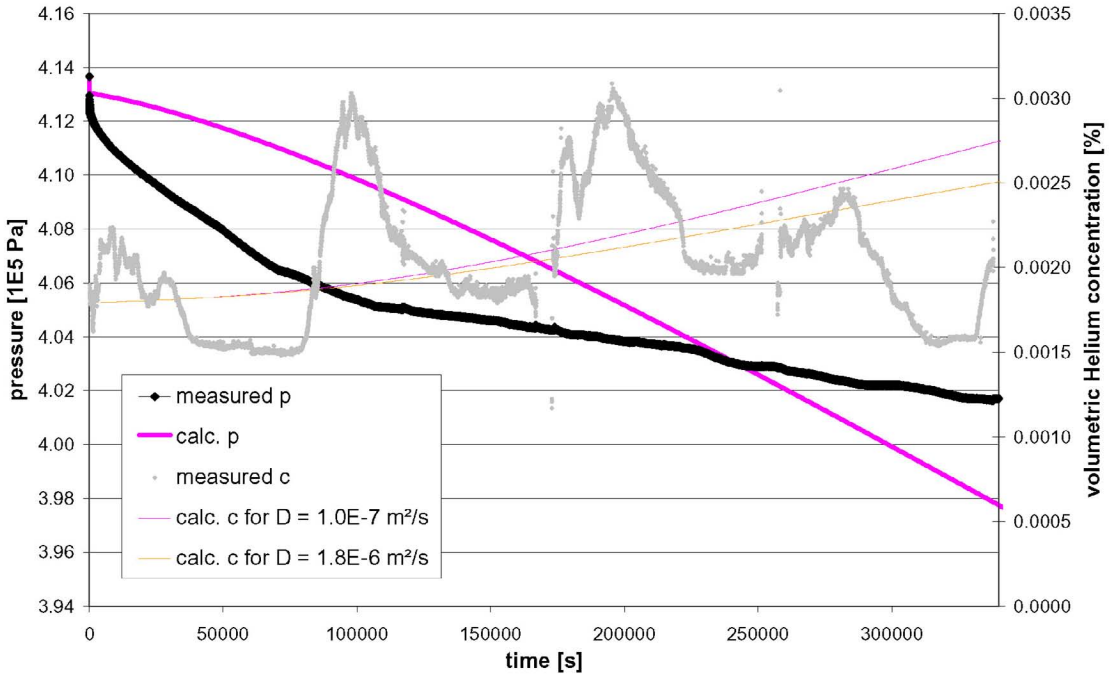

Figure 5-16. *Results for tracer test on PA3473A01: variation of diffusion coefficient.*

Figure 5-17 shows the influence of gas saturation. The permeability value in the calculations was 10^{-21} m^2, the diffusion coefficient was 10^{-7} m^2/s. The bold pink line is for pressure in the calculation with a gas saturation of 0.2%, the bold dark blue line for a gas saturation of 0.05%. The thin lines are for the corresponding volumetric Helium content of the gas flow into the sensor hose line; for this value the calculations gave no significant difference for this test configuration.

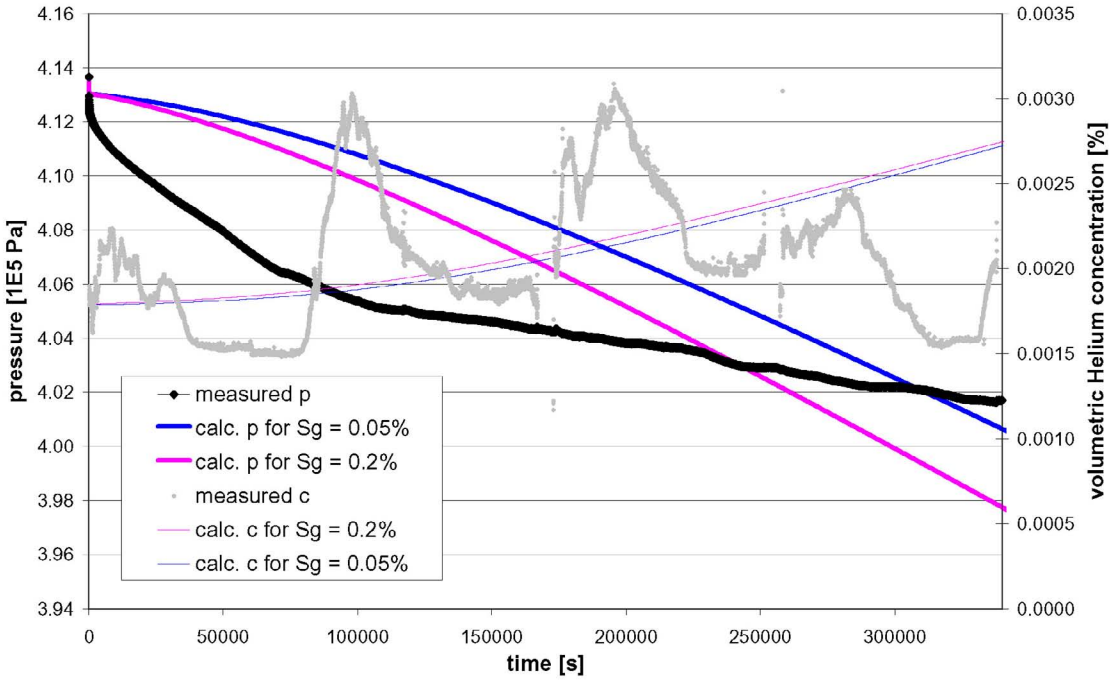

Figure 5-17. *Results for tracer test on PA3473A01: variation of gas saturation.*

For the test on location PA3474A01 Figure 5-18 shows a comparison between measured and calculated data (diffusion coefficient 10^{-7} m^2/s, gas saturation 2.5%) for permeability values of $7 \cdot 10^{-21}$ m^2 (pink lines) and 10^{-21} m^2 (dark blue lines).

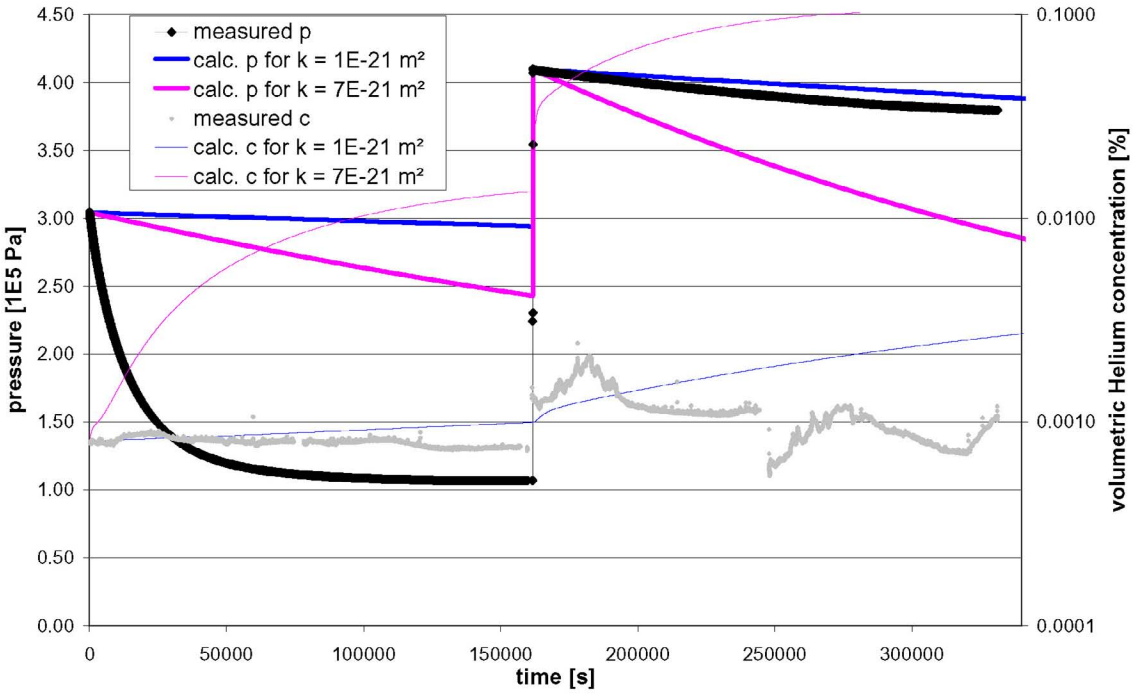

Figure 5-18. *Results for tracer test on PA3474A01.*

The description of the hydraulic behaviour (compare also the surface packer / mini packer test with gas, Figure 5-6) of location PA3474A01 demands not only further investigation of the location itself but also a numerical hydraulic model beyond a simple, homogeneous porous medium (for example dual-continuum model for micro-cracks in porous medium). The exact description of the very specific hydraulic behaviour of this test position is not within the scope of this work.

6 Observations

Beneath the measurements of permeability and the gas tracer tests that are reported in chapter 5 there had been some measurements on test locations with natural fractures in the A-tunnel with gas. These tests have not been reported in the earlier documents, because there had been leakages directly at the surface packer so that an analysis of these tests with respect to permeability was not possible. Nevertheless, during these tests interesting observations were made that give a feeling for the heterogeneity of the excacation damaged zone in crystalline rock.

One of these tests was performed on location PA3483A01. When the leakage at the surface packer was detected (bubbles observed with leak detector spray) also the gallery wall around the test location was sprayed. The photos in Figure 6-1 and Figure 6-2 show clearly the effect of channeling in the natural fractures: Though the outline of the fracture could be observed along the gallery wall, the gas came out from the fracture only on few positions. Another finding in this test was that the gas came out of the gallery wall also on positions where no fractures or cracks were visible before. Notice in the photo the folding rule (2 m) on the red cable.

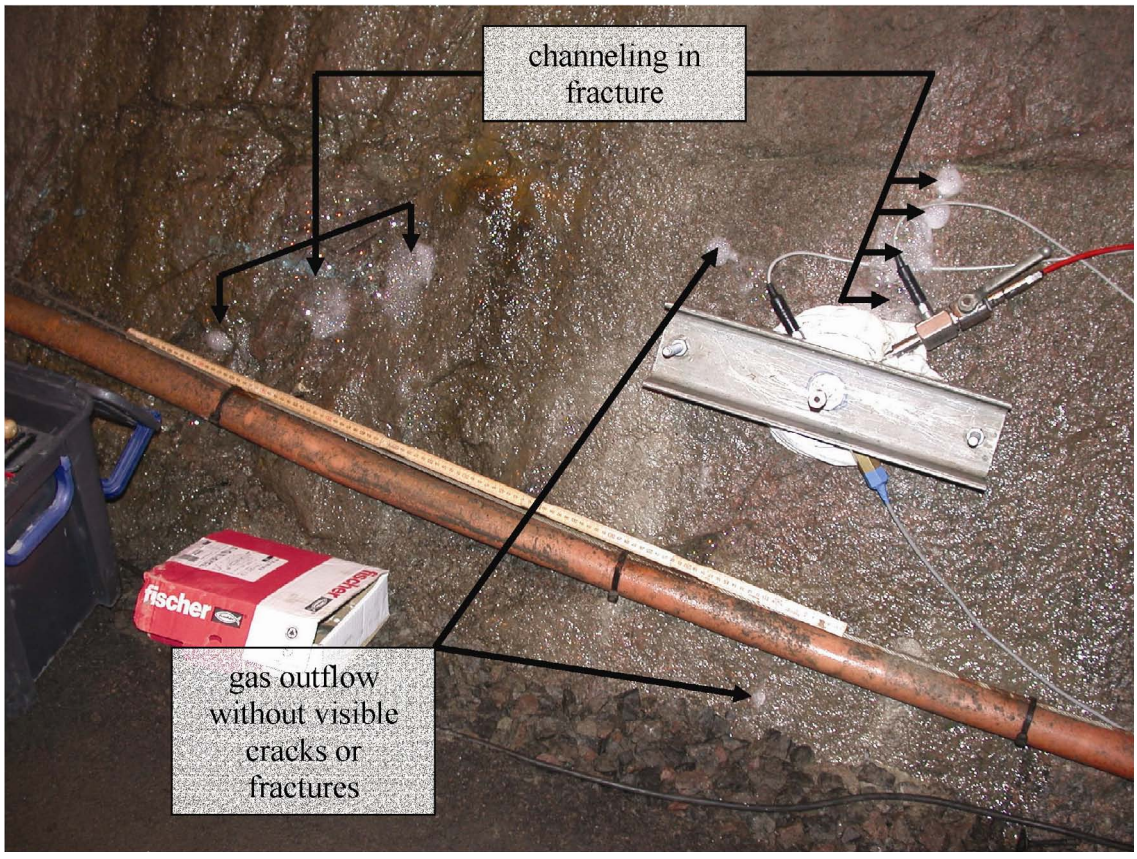

Figure 6-1. *Observation from test with gas in the A-tunnel on PA3483A01 in total view.*

Figure 6-2. *Observation from test with gas in the A-tunnel on PA3483A01 in detailed view.*

7 Discussion

The permeability values that have been derived from the surface packer tests described in this report are based on the comparison of measured and calculated pressure at the end of the test. These values do not indicate a cohesive network of microcracks in the rock matrix, but this does not mean that such networks nowhere exist (compare chapter 6).

For the early time period of the tests the measured pressure drop was quicker, which can be seen even more clearly in the pressure derivative (see plots in Figure 5-2 and Figure 5-7). This can be explained by dead-end microcracks with slightly increased permeability that are connected to the testing volume, but not connected to a cohesive network that forms a pathway between the open gallery wall (or the natural fracture network) and the testing volume.

For comparison Figure 7-1 shows a compendium of the in situ and laboratory results from the ZEDEX-project (EMSLEY et al. 1997) together with the results from BGR's surface packer tests. The x-axis indicates the begin and end of the tested interval in the ZEDEX-boreholes. In the case a test resulted in an upper and lower limit for the measured permeability (y-axis) value, this result appears as a rectangle in this diagram. The permeability values are classified with respect to the excavation methods.

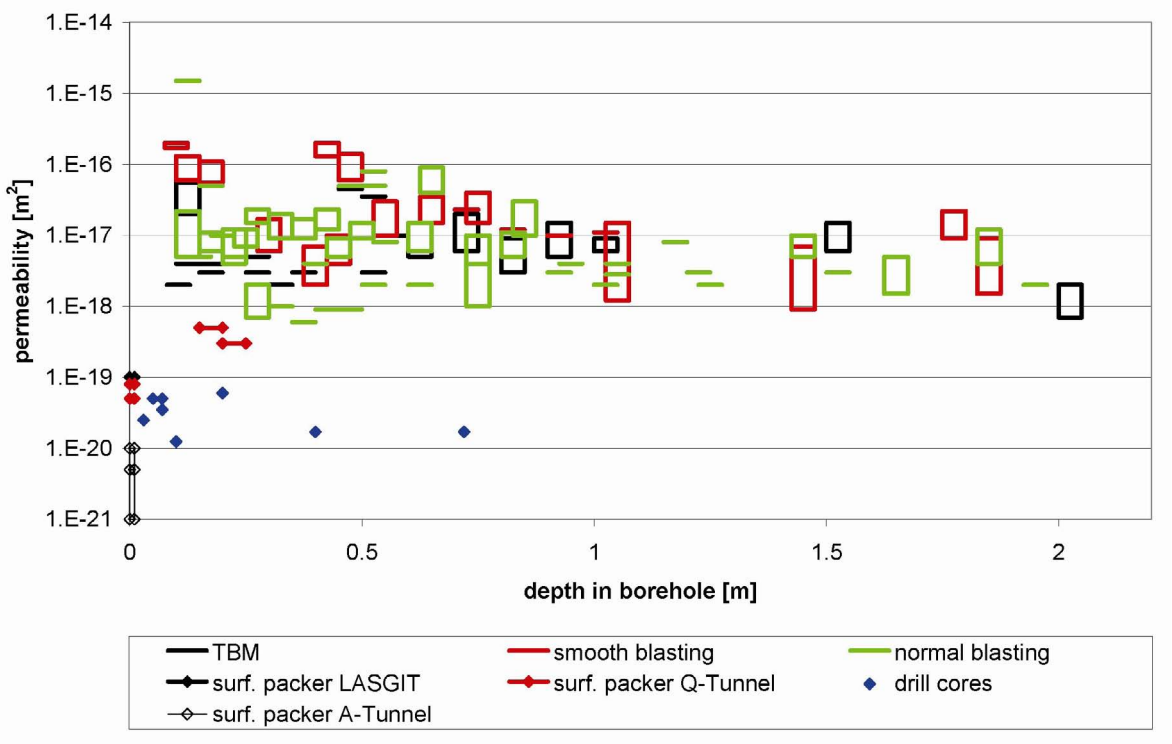

Figure 7-1. *Compendium of measured permeabilities in situ from the ZEDEX-project (data from EMSLEY et al. 1997).*

The comparison of the permeabilities measured with the surface packer system and results from the ZEDEX-project emphasize together with the observations described in chapter 6 the importance of considering the scale when interpreting a permeability value. Though the test locations of the surface packer tests were directly on the gallery's surface (where usually most damage from excavation is expected) the measured permeability values are in the range of the values from laboratory experiments on drill cores.

In the surface packer / mini packer test in the TBM-excavated A-tunnel a gas entry pressure (within test duration) of about 1 MPa or more was found (compare chapter 5.3.1). MARSCHALL et al. (1999) found in laboratory experiments on samples of rock matrix from the Grimsel Test Site that the two-phase flow model of BROOKS & COREY (1964) fitted best with measured data with the following parameter values: gas entry pressure between 0.4 MPa and 0.8 MPa, residual gas saturation 0.0, residual water saturation between 0.4 and 0.45, and parameter λ between 0.7 and 2. With respect to gas entry pressure the value found with the surface packer / mini packer tests is in the same order of magnitude as the experimental findings from MARSCHALL et al. (1999) for the rock matrix.

The interpretation of the gas tracer tests is tainted with uncertainty for several reasons. The comparison of the measured evolution of volumetric Helium content of the gas flow into the detector with the evolution of pressure in the gallery (compare Figure 5-9 and Figure 5-11) indicate a dependence of these values: rising values of measured Helium content coincide more or less with falling values of pressure in the gallery. The Helium detector has to be operated at nearly zero overpressure (compare chapter 3). The measured gas flow was a mixture of gas from the gallery and gas from the packer whereas the apportionment remains unknown. For this reason the measured Helium concentration cannot be analysed with respect to a recovery value, a common value in the analysis of tracer test.

Nevertheless measured and calculated data for test location PA3473A01 can be interpreted as a confirmation that the range of parameter values derived from BGR's permeability tests are reasonable. Calculations of the tracer tests with higher permeability values than measured would result in strong deviations not only with respect to the pressure evolution in the borehole but also even more pronounced in the calculated volumetric Helium concentration of the gas flow into the detector (compare Figure 5-15).

8 Summary

For the hydraulic characterization of the excavation damaged zone BGR has developed surface packer systems. This packer type is fixed directly on the gallery wall, for this reason it is very qualified as a tool to characterize the area that is most damaged by excavation where borehole packers are not applicable.

In crystalline formations the movement of water and gas takes place mainly on natural fractures or (micro-)cracks. In the vicinity of a cavity the generation of (micro-)cracks is determined by the mechanical behaviour of the formation, the initial stress field, and the method of excavation. The surface packer systems were used in the HRL Äspö in galleries that were excavated by drill and blast and by TBM, also in deposition holes. Water, air, and Helium were used as test fluid.

Hydraulic tests were conducted mainly on test locations were no fracture or crack was visible. The permeability values that have been derived from these tests are based on the comparison of measured and calculated pressure at the end of the test. These values do not indicate a cohesive network of microcracks in the rock matrix, but this does not mean that such networks nowhere exist: especially in one test (which has not been evaluated with respect to a permeability value due to a leakage) gas flow in microcracks was observed. For the early time period of the tests the measured pressure drop is quicker, which can be seen even more clearly in the pressure derivative. This can be explained by dead-end microcracks with slightly increased permeability that are connected to the testing volume, but not connected to a cohesive network that forms a pathway between the open gallery wall (or the natural fracture network) and the testing volume.

The analysis of gas tracer tests requires the provision for two-phase flow and transport. The necessary parameter values were taken on the one hand from the surface packer tests, on the other hand from literature data. The multitude of parameter values, but also the measuring technique cause uncertainties in the interpretation of the gas tracer tests. Nevertheless, the comparison between measured and calculated data can be interpreted as a confirmation that the parameter values that were used for flow and transport in the calculation are reasonable.

9 References

Bredehoeft, J.D. & Papadopulos, I.S. (1980): A Method for Determining the Hydraulic Properties of Tight Formations. Water Resour. Res., 1 (16), 233 – 228.

Brooks, R. H. & Corey, A. T. (1964): Hydraulic Properties of Porous Media.- Colo. State Univ., Hydrol. Pap., 3; Fort Collins (USA).

Cooper, H.H, Bredehoeft, J.D. & Papadopulos, I.S. (1967): Response of a Finite-Diameter Well to an Instantaneous Charge of Water. Water Resour. Res., 3 (1), 263 – 269.

Emsley, S., Olsson, O., Stenberg, L., Alheid, H.-J. & Falls, S. (1997): ZEDEX - A Study of damage and disturbance from tunnel excavation by blasting and tunnel boring. Svensk Kärnbränslehantering AB, Technical Report 97-30: 198 p., 96 fig., 28 tab.; Stockholm.

Hardenby, C. (2004): Large Scale Gas Injection Test - The LASGIT hole DA3147G01 Hydrogeology. Svensk Kärnbränslehantering AB, International Progress Report IPR 04-52: 59 p., 34 fig., 17 tab.; Stockholm.

Maaranen, J., Lehtioksa, J. & Timonen, J. (2001): Determination of Porosity, Permeability and Diffusivity of rock samples from Äspö HRL using the Helium gas method. Svensk Kärnbränslehantering AB, International Progress Report IPR 02-17: 37 p., 23 fig., 5 tab., 3 app.; Stockholm.

Marschall, P., Fein, E., Kull, H., Lanyon, W., Liedtke, L., Müller-Lyda, I. & Shao, H. (1999): Conclusions of the Tunnel Near-Field Programme (CTN). NAGRA, Technical Report 99-07: 120 p., 45 fig., 17 tab.; Wettingen (Schweiz).